UNIVERSITY OF CALIFORNIA
RIVERSIDE

Cellular Responses to Different Types of Mitochondrial DNA Damage

A Thesis submitted in partial satisfaction
of the requirements for the degree of

Master of Science

in

Environmental Toxicology

by

Ching-Hsin Yang

September 2022

Thesis Committee:
Dr. Linlin Zhao, Chairperson
Dr. David Volz
Dr. Yinsheng Wang

The Thesis of Ching-Hsin Yang is approved:

_____

_____

_____

Committee Chairperson

University of California, Riverside

ABSTRACT FOR THE THESIS

Cellular Responses to Different Types of Mitochondrial DNA Damage

by

Ching-Hsin Yang

Master of Science, Graduate Program in Environmental Toxicology
University of California, Riverside, September 2022
Dr. Linlin Zhao, Chairperson

Mitochondrial DNA (mtDNA) is a circular DNA molecule existing in multiple copies in mitochondria. mtDNA contains a higher level of chemical-induced DNA lesions than nuclear DNA due to the accumulation of lipophilic and charged chemicals in the mitochondria and the lack of certain DNA repair pathways. mtDNA lesions can alter mitochondrial function, such as the reduction of mitochondrial respiration, mitochondrial membrane potential and an elevation of mitochondrial reactive oxygen species (ROS). In response to mtDNA damage, DNA repair, mtDNA degradation and mitochondrial dynamics are the major pathways to eliminate mtDNA damage. The relative contributions of mtDNA repair, degradation, and mitochondrial dynamics in response to different types of mtDNA damage remains an outstanding question. To address this question, characterizing these pathways in mtDNA damage cell models was conducted in this study. First, inducible mitochondrial targeting uracil DNA glycosylase 1 variant (UNG1-Y147A) transduced HeLa and HEK293 cells with APE1 siRNA transfection

were used as mitochondrial abasic site (AP) lesion models. The mtDNA copy numbers were significantly reduced in the UNG1-Y147A-overexpressed HeLa and HEK293 cells. However, PCR-blocking lesions on mtDNA were not increased in the UNG1-Y147A-overexpressed or *APE1*-knockdown cells. DNA repair and mitochondria dynamics-related genes were not significantly altered. mtDNA degradation was the main response in the mtDNA AP lesion models. Second, mitochondrial targeting chemical mt-Ox was used to generate mtDNA oxidative damage in HeLa and HEK293 cells. Different from UNG1-Y147A, mt-Ox increased PCR-blocking lesions on mtDNA without reducing mtDNA copy number. mt-Ox also induced the expressions of DNA repair and mitochondria dynamics-related genes in HeLa cells. DNA repair and mitochondria dynamics were more significant in response to mtDNA oxidative damage. The difference in response might be due to the types and amounts of lesions. The mechanisms of damage response activation and decision need further investigation. In conclusion, this study provides solid evidence that cells had different damage responses in the mtDNA AP lesions and oxidative damage models. The evidence provides insights into different cellular responses to different types of mtDNA lesions and guides future research for illustrating the mtDNA damage induced adverse outcome pathways.

Table of Content

List of Tables

List of Figures

1 Introduction

1.1 Mitochondrial Toxicity

The mitochondrion is an important organelle for energy production, steroidogenesis, calcium regulation, regulation of apoptosis and cell signaling[35]. The integrity of mitochondria is important for human health since multiple diseases, such as cancer and neurodegeneration, have been associated with mitochondrial dysfunction and oxidative damage[8]. Some chemicals have been reported to induce mitochondrial toxicity and cause physiological disorders. For example, rotenone is an electron transport chain complex I inhibitor that increases reactive oxygen species (ROS) production in mitochondria and induces apoptosis[40]. Antimicrobial agent triclosan can increase ROS levels, depolarize mitochondrial membrane potential, and disrupt mitochondrial structure in mammalian cell lines[55]. Trivalent arsenic (Arsenite) has been reported to alter pyruvate metabolism, reduce ATP-linked respiratory capacity, and increase proton leak in *C. elegans* (*Caenorhabditis elegans*)[27]. Furthermore, emerging pollutants, including phthalates, fungicides, and flame retardants, have been identified as mitochondrial toxicants with uncertain modes of toxicity[28]. To understand the possible adverse effects of these emerging pollutants, investigating the modes of mitochondrial toxicity are required.

1.2 Mitochondrial DNA

Mitochondrial DNA (mtDNA) is a closed circle double-stranded DNA located in mitochondria. The sense strand and antisense strand of mtDNA are named as heavy

(H) strand and light (L) strand. In human cells, mtDNA contains 16,569 base pairs and encodes 22 tRNAs, two ribosomal RNAs and 13 protein subunits of oxidative phosphorylation (OXPHOS) complexes. Besides coding sequence, mtDNA contains a noncoding displacement loop (D-loop) which is important for mtDNA replication and transcription[52, 60]. One mitochondrion contains multiple copies of mtDNA, but the mtDNA copy number varies in different cell types and developmental stages[46]. Since there are multiple copies of mtDNA within each cell, some copies can carry mutated sequences without affecting cell physiology. The situation in which two or more mtDNA variants exist within a cell is called heteroplasmy[47]. The selection of healthy copies for heritage is crucial for oocyte development[9, 24].

Different from nuclear DNA (nDNA) which is wrapped by histones, mtDNA is packaged by other proteins, such as mitochondrial transcription factor A (TFAM), DNA polymerase gamma (POLG), and twinkle (TWNK), and forms mtDNA-protein complexes termed mitochondrial nucleoids[60]. As one of the most abundant nucleoid proteins packaging mtDNA into nucleoids, TFAM regulates mitochondrial transcription and mtDNA replication as well. Knockdown of *tfam* in zebrafish (*Danio rerio*) embryos causes mtDNA copy number reduction, OXPHOS deficiency and developmental abnormalities[32]. Homozygous *Tfam*-knockout mice are embryonic lethal with significant mtDNA loss[21]. TFAM is essential for mtDNA maintenance and mitochondria integrity.

1.3 Mitochondrial DNA Damage

mtDNA contains more chemical-induced lesions than nuclear DNA due to the accumulation of lipophilic and charged chemicals in mitochondria and the absence of certain DNA repair pathways[64]. For example, the abundance of mtDNA lesions increases significantly in the blood and skeletal muscle of the rats after five daily 3.0 mg/kg/day rotenone injections. However, nDNA damage is not observed in either tissue[41]. Compared to nDNA, mtDNA is more vulnerable. But the understanding of mtDNA damage lags behind that of its nuclear counterpart.

The removal of the nitrogenous base causes the formation of absic sites (AP sites). AP lesion is one of the most abundant DNA lesions in mitochondria and nucleus. The steady-state amount of AP sites is approximately 30,000 per cell[48]. AP sites arise from a variety of chemical and biochemical processes including the loss of unstable modified nucleobases, intermediates generated by DNA glycosylases and free radical attack on deoxyribose. Accumulation of AP sites would cause secondary DNA damages, such as DNA-protein crosslinks (DPCs) and DNA strand breaks[37]. DPC is a severe type of nuclear DNA damage to cause sister chromatid exchanges, transformation, and cytotoxicity[1]. In mitochondria, AP lesions are also abundant and can number in the hundreds per cell[59]. Besides forming DPCs and DNA strand breaks, the accumulation of mitochondrial AP sites triggers mtDNA degradation in human cell lines and mice[22, 44]. The reduction of mtDNA copy number can cause OXPHOS deficiency and mitochondrial membrane potential depolarization[45]. Therefore, AP lesion is more harmful to mitochondria.

DNA oxidation is one of the common base modified lesions, such as 8-oxoguanine (8-oxoG) and 8-oxoadnine. 8-oxoG is the most common oxidative lesion since guanine has the lowest reduction potential among the four nitrogenous bases. The steady-state amount of 8-oxoG is about 2,400 per cell[48]. ROS are the major oxidants of DNA oxidation. Therefore, 8-oxoG is widely used as a biomarker of oxidative stress[7]. 8-oxoG can be removed by base excision repair (BER) which is initiated by 8-oxoG glycosylases, such as 8-oxoguanine DNA glycosylase-1 (OGG1) and mutY DNA glycosylase (MUYTH)[16]. During DNA replication, 8-oxoG can pair with adenine to cause transversion mutations[7]. 8-oxoG is a mutagenic DNA lesion. mtDNA locates in the mitochondrial matrix where most cellular ROS are generated, so mtDNA accumulates more oxidative damage than nDNA[52]. Interestingly, the elevation of oxidative damage doesn't increase the mutation rate of mtDNA in mice and mammalian cell lines[16, 43]. Mitochondria might equip novel mechanisms to protect mtDNA against oxidative damage induced mutation. Other types of mtDNA damage are also detected in biological samples, such as DNA double strand breaks and DNA adducts[52]. Although various types of mtDNA damage are found in cells, the cellular responses to different types of mtDNA damage are unclear.

1.4 Mitochondrial DNA Damage Responses

DNA repair is an important process for removing DNA damage in mitochondria. Base excision repair (BER) is the most characterized pathway in mitochondria. BER removes various types of DNA lesions, including uracil, oxidized bases, and

deaminated and hydrolyzed bases. In BER, different glycosylases remove targeted DNA lesions to become AP sites and AP endonuclease 1 (APE1) cut the AP sites to form 5'-deoxyribose phosphates (5'-dRPs). Then 5'-dRPs are processed by short-patch BER, in which POLG fills the gaps and DNA ligase 3 (LIG3) seals the nicks to complete the repair. Alternatively, in long-patch BER, POLG inserts more than one nucleotide and flap endonuclease 1 (FEN1), DNA Replication Helicase/Nuclease 2 (DNA2) and Exo/Endonuclease G (EXOG) remove the flaps before LIG3 sealing the DNA nicks[11, 12]. In contrast, nucleotide excision repair (NER) is absent or inefficient in mitochondria. Whether other DNA repair pathways exist in mitochondria, such as mismatch repair (MMR) and homologous recombination (HR), are still controverisal[11].

Multiple copies of mtDNA allows mitochondria to remove DNA damage by degrading damaged molecules. mtDNA degradation seems to be an essential tool to remove overwhelming oxidative and alkylating damage which is beyond the repair capacity[43], and also eliminate some types of DNA damage that are not able to be repaired in mitochondria, such as ultraviolet light-induced pyrimidine dimers and DNA DSBs[12, 18]. For restriction-enzyme-induced mtDNA DSBs, instead of being repaired, broken mtDNA are rapidly degraded, leading to a significant drop in copy number[12]. Although mtDNA degradation has been observed in many mtDNA damage models, the mechanisms and regulations of mtDNA degradation are still unclear. The stalling of replication or transcription complexes is a likely to be a trigger of mtDNA degradation[18]. Endonuclease G (ENDOG) is an abundant nuclease

in mitochondria, which is thought to degrade damaged mtDNA[15]. On the other hand, recent studies show that mtDNA replication complex proteins, POLG, TWNK and Mitochondrial genome maintenance exonuclease 1 (MGME1), play roles in both mtDNA replication and the degradation of mtDNA with DSBs in HEK293 cells[34]. Furthermore, mtDNA degradation deficiencies are observed in *Polg* mutant mice and *Mgme1*-knockout mice[29, 30]. Besides coating on mtDNA, regulating transcription and DNA transactions in mitochondria, our laboratory proposes that TFAM may play a role in mtDNA degradation. Our results show that TFAM forms Schiff base intermediates with damaged DNA at AP sites and accelerates strand cleavage *in vitro*[59]. However, the subsequent pathways to degrade the cleaved mtDNA remain to be clarified.

Mitochondria dynamics include mitochondria fission and fusion. Mitochondria fusion is the event that two adjacent mitochondria fuse into one mitochondrion coordinated by mitofusin 1 (MFN1), mitofusin 2 (MFN2) located in the outer mitochondrial membrane (OMM) and optic atrophy 1 (OPA1) in the inner mitochondrial membrane (IMM). On the other hand, mitochondria fission in which OMM-bound proteins, such as mitochondrial fission 1 (FIS1) and mitochondrial fission factor (MFF), recruit dynamin-related protein 1 (DRP1) to separate one mitochondrion into two[25]. A previous study reported that mitochondrial fission/fusion and mitophagy genes were required for removing UV-induced mtDNA lesions in *C. elegans*[3]. Another study indicates that acrolein significantly increases mtDNA damage, reduces mtDNA copy number and induces mitochondrial fission

and mitophagy in human cell lines[53]. Therefore, mitochondrial dynamics and mitophagy are considered possible mtDNA damage response pathways.

Although some mtDNA damage responses have been identified, the contribution and coordination of these processes to eliminate damage are unclear. Furthermore, cells might have different damage response contributions to different types of damage. Therefore, clarifying the interactions between damage response pathways and different mtDNA damage is crucial for plotting mtDNA damage initiated adverse outcome pathways.

1.5 Adverse Effects of Mitochondrial DNA Damage

Codon alterations, such as DNA mutation and carcinogenesis, are the most documented outcomes of DNA damage. Several mtDNA mutations and the associated diseases have been identified as well. Kearns–Sayre syndrome which is associated with progressive myopathy, ophthalmoplegia, and cardiomyopathy is caused by mtDNA deletions. Leber's hereditary optic neuropathy is an optic neuropathy that is caused by mtDNA point mutations[60]. Recent studies also show that mtDNA mutations are associated with other chronic diseases, including diabetes, Alzheimer's disease, and Parkinson's disease[60]. Therefore, preventing mtDNA mutations is crucial for human health.

mtDNA damage induced copy number reduction causes mitochondrial physiology alteration as well. The respiration rates, mitochondrial membrane potentials and ROS production are significantly reduced in three different mtDNA

depleted cell lines[45]. On the other hand, the reduction of embryonic mtDNA copy number doesn't cause malformation in the newborn mice but increases hepatic lipidosis and induces glucose intolerance at five months of age[54].

mtDNA damage also causes cellular physiology alteration unrelated to codons. For example, damaged mtDNA can be an immune signaling molecule to induce pro-inflammatory and type I interferon (IFN) responses[56]. A previous study found that low-level and prolonged oxidative stress generated by glucose oxidase reduced the mtDNA integrity and copy number in BEAS2B cells. Following that, the damaged mtDNA molecules enter the cytoplasm and bind to Z-DNA binding protein 1 (ZBP1) to trigger inflammation[49]. A recent study shows that oxidized mtDNA is cleaved by FEN1 and transported out of mitochondria via mitochondrial permeability transition pore and voltage-dependent anion channels (VDACs) to activate leucine-rich repeat protein-3 (NLRP3) inflammasome and stimulator of interferon genes (STING)[58]. The other study also discovers that mtDNA DSBs can induce the release of mitochondrial RNA to cytoplasm and trigger both IFN response and retinoic acid-inducible gene I (RIG-I) - mitochondrial antiviral-signaling protein (MAVS) dependent immune response[50]. Plenty of evidence indicates that mtDNA damage can cause various adverse effects in different cells and organisms. However, a complete picture connecting mtDNA damage (Molecular initiating event), mitochondrial dysfunction (Key event) and physiological alteration (Adverse outcome) is missing.

1.6 Mitochondrial Targeting Uracil DNA Glycosylase 1 Variants

Uracil DNA glycosylase 1 (UNG1) is a DNA repair enzyme which removes uracil to form AP sites in DNA and initiates the BER pathway. *In vitro* enzyme activity experiments show that UNG1-Y147A and N204D variants can generate excessive AP sites from thymine and cytosine, respectively[17]. Based on the excessive glycosylase activities of the UNG1 variants, mitochondrial targeting UNG1 variants are introduced to generate mtDNA specific AP lesions in cell and animal models. Overexpression of mitochondrial targeting UNG1-Y147A variant in mouse hippocampal neurons significantly reduces mtDNA copy number and transcription activities, and increases oxidative stress in hippocampus[22]. The following study also indicates that the overexpression of UNG1-Y147A in mouse cardiac myocytes decreases the mtDNA copy number, mtDNA encoded transcripts and mitochondrial respiration rate in the heart tissues. In contrast, mitochondrial mass, antioxidative defense enzymes, and mitochondrial fission/fusion gene expressions are induced in the heart tissues[23]. Overexpression of mitochondrial targeting UNG1-Y147A and -N204D variants significantly reduce the mtDNA copy numbers. However, A>G (T>C) transition or A>T (T>A) transversion mutations are not increased in mtDNA. On the other hand, G>A (C>T) mutation in mtDNA is increased in the cells expressing UNG1-N240D variant but not in the cells expressing the UNG1-Y147A variant[20]. Overall, mtDNA copy number reduction is the most iconic phenomenon of mitochondrial targeting UNG1 variants overexpression.

1.7 Mitochondrial Targeting DNA Damage Agents

To investigate the cellular responses to mtDNA damage, inducing mtDNA specific damage *in vivo* is required but challenging. To achieve this aim, some mitochondrial targeting chemicals have been developed. MitoParaquat which is a triphenylphosphonium lipophilic cation conjugated paraquat can significantly increase the mitochondrial ROS level in C2C12 cells[39]. A light activated system, Mito-FAP–MG-2I complex, can produce singlet oxygen in mitochondria[36]. Kelly and colleagues developed a series of mitochondria-penetrating peptides (MPPs) linked DNA-damaging agents to induce different types of lesions specifically on mtDNA, such as mt-cbl (Chlorambucil)[10], mt-Dox (Doxorubicin)[4] and mt-Ox[57]. mt-Ox is a mitochondrial targeting DNA oxidizing agent which can induce 8-oxoguanine in mitochondria rather than nucleus. The PCR-blocking DNA lesions are also presented on mtDNA but not on nDNA. mt-Ox is able to induce mtDNA oxidative damage specifically with low off-target effects[57].

1.8 Objectives

mtDNA damage is a molecular initiating event that affects hallmarks of mitochondrial dysfunction, which can lead to adverse outcomes for higher endpoints[8]. Some possible mtDNA damage responses have been documented, but the contributions of these responses to eliminate different types of mtDNA damage are not clear. Therefore, the aim of this study is exploring the contributions of mtDNA damage responses, including mtDNA repair, mtDNA degradation and mitochondrial

dynamics, against different types of mtDNA damage in cells. To investigate the cellular responses to different mtDNA lesions in human, human cell lines, HeLa and HEK293 cells, with mitochondrial targeting UNG1-Y147A variants and APE1 siRNA transfection were used as the mitochondrial AP lesion cell models. On the other hand, HeLa and HEK293 cells with mitochondrial targeting chemical mt-Ox treatment were defined as the mtDNA oxidative damage cell models in this study. mtDNA degradation was monitored by counting mtDNA copy numbers through qPCR. mtDNA repair and mitochondrial dynamics were validated by the expressions of mtDNA repair and mitochondrial dynamics-related genes. Overall, this study provides insights into pathways and different damage responses.

2 Materials and Methods

2.1 Cell Lines

Human cell lines, HEK 293T cell line, tet-on HeLa cell line, and HEK 293 Tet-On® 3G Cell Line (Takara Bio USA, 631185), were cultured in Dulbecco's Modified Eagle Medium (DMEM) (Gibco, 12100-046) supplemented with 10% Tet System Approved Fetal Bovine Serum (Takara Bio USA, 631106) in the presence of 5% CO_2 at 37℃.

2.2 Lentivirus Transduction

HEK293T cells were seeded in 6-well plates one day before lentiviral plasmids transfection. 1.5 μg lentiviral transfer plasmid (pMA-3287 UNG1-Y147A (Addgene, 46883), pMA3288 UNG1-WT (Addgene, 46885), or pMA2780 UNG1-N204D (Addgene, 25438)), 1 μg packaging helper plasmid psPAX2 (Addgene, 12260) and 0.6 μg envelop helper plasmid pmD2.G (Addgene, 12259) in 87.6 μL water were mixed with 12.4 μL 2 M $CaCl_2$ and 100 μL 2x HBS (pH 7.0, 50 mM HEPES, 280 mM NaCl, and 1.5 mM Na_2HPO_4) and incubated at room temperature for 15 min. After incubation, the transfection mixture was added to the cells dropwise. Cell medium was renewed at the 24^{th} hr after transfection and collected after another 24^{th} hr. The collected cell medium was centrifuged (500g, 10 min) at 4°C to remove suspended cells and cell debris. One volume of Lenti-X™ Concentrator (Takara Bio, 631231) was mixed with three volumes of cell medium supernatant and incubated at 4℃ overnight. To collect lentivirus, the mixture was centrifuge at 1,500g for 45

minutes at 4°C. Lentivirus in the pellet was resuspended in 1/10 of the original volume of DMEM after removing the supernatant.

Host cells (tet-on HeLa or tet-on HEK293) were mixed with different dilutions of lentiviral suspensions and seeded into a 6-wells plate. One day after transduction, lentiviral suspensions were replaced by selection media to eliminate non-transduced cells. The selection medium was renewed daily until the well of cells without lentivirus transduction was wiped out. The surviving cells were transferred to T25 flasks for expansion. After the cell number expansion, a portion of the cells was collected for draft genotyping and transduced gene expression analysis by Western blot, and the remaining cells were stored in liquid nitrogen.

For transduced gene expression analysis, transduced cells were seeded in 10-cm cell culture dishes. When the cell confluency reached 60%, culture media were replaced by DMEM with 0.5 μg/mL Doxycycline (DOX). After 24 hr induction, cells were collected for Western blot.

After the draft genotyping and transduced gene expression analysis, transduced cells were trypsinized for single colony selection. First, cells were diluted into 10,000 cells/mL suspension and added into the first columns of a 96-well plate. Cell suspensions were serially diluted by two-fold from the first columns to the last columns. After the cell number expansion, wells with single colonies were selected as the stable colonies of the cell line. At least two stable colons are selected in one cell line.

2.3 Genotyping

Total DNAs of transduced cells were extracted by Monarch® Genomic DNA Purification Kit (New England Biolabs, T3010) following the manufacturer's instruction. The transduced sequences in the genomic DNAs were amplified by Phusion® High-Fidelity DNA Polymerase (New England Biolabs, M0530S) through the PCR reactions and purified by DNA Clean & Concentrator™-5 (Zymo Research, D4004) after the PCR reactions. The purified PCR products were sequenced by Sanger sequencing.

2.4 siRNA Transfection

Two days before small interfering RNA (siRNA) transfection, HeLa or HEK293 cells were seeded in 10-cm cell culture dishes. One hour before transfection, cells were replenished with fresh DMEM. To knockdown APE1 expression, cells were transfected with 100 pmol of ON-TARGET plus human APEX1 siRNA (Dharmacon, J-010237-08-0002) or 100 pmol of ON-TARGET non-targeting siRNA pool (Dharmacon, D-001810-10-05) as the negative control using Lipofectamine® RNAiMAX Reagent (Invitrogen, 13778-150). After 72 h upon transfection, cells were collected and freeze by liquid nitrogen.

For APE1 knockdown and UNG1 induction co-treatment, cells (tet-on HeLa with UNG1-Y147A or tet-on HEK293 UNG1-Y147A) in 10-cm dishes were transfected with human APEX1 or non-targeting siRNA and supplemented with doxycycline (Final concentration in the media: 0.5 μg/mL) at the 48^{th} hr after

transfection. Finally, cells were collected after 24 hr doxycycline induction (72 hr after transfection).

2.5 mt-Ox Treatment

mt-Ox was a kind gift from Dr. Shana Kelly. The preparation and characterization of mt-Ox have been documented in Wisnovsky *et al*., 2016[57]. For Lethal Concentration, 50% (LC_{50}) determination, cells (HeLa or HEK293) were treated with different mt-Ox dosing DMEM (48, 24, 12, 6, 3 and 1.5 μM) or vehicle control (0.5% DMSO) in 96-well plates. After 1 hr incubation in the cell incubator, cells were exposed to visible light for 10 min to induce mt-Ox emitting singlet oxygen in response to light in the visible range. Cell viabilities were measured by Cell Counting Kit-8 (CCK-8) (Dojindo Molecular Technologies, CK-04) at the 24th and 48th hr after light activation.

For cell response monitoring, cells were treated with 3 or 6 μM mt-Ox dosing media or vehicle control (0.1% DMSO) media in 10-cm dishes and 96-well plates. At the 8th, 24th, and 48th hr after light activations, cells in 10-cm dishes samples were collected for further experiments and cells in 96-well plates were used for cell viability measurements.

2.6 Western Blot

For extracting crude mitochondrial fraction, cell pellets were resuspended in 1 mL Cytosol Extraction Buffer (30 mM HEPES, pH 7.4, 1 mM EDTA, 1 mg/mL BSA and 320 mM Sucrose) and incubated on ice for 10 min. After incubation, cell suspensions were homogenized with a Dounce-Grinder and transferred to a centrifuge tube for low-speed centrifugation (1200g, 5 min). Supernatants were collected and centrifuged again. The new supernatants were centrifuged at 15,000g for 10 min. Pellets were resuspended in 1 mL Cytosol Extraction Buffer and centrifuged at 15,000g for 10 min again. The final pellets were resuspended by 100 μL PBS as the crude mitochondrial fraction. The protein concentrations of the crude mitochondrial fractions were measured by Pierce™ Rapid Gold BCA Protein Assay Kit (ThermoFisher Scientific, A53225).

Protein samples were mixed with ¼ volume of 5x loading buffer (10% SDS, 250 mM Tris Base, 0.02% Bromophenol Blue, 5% Beta-mercaptoethanol and 30% Glycerol) and heated at 95ºC for 5 min. Denatured protein samples were separated in the SDS-PAGE gels and transferred to nitrocellulose membrane for blotting. Newly transferred membranes were blocked in the blocking solution (5% BSA, 20 mM Tris, pH 7.5, 150 mM NaCl and 0.1% Tween 20) for 1 hr. After blocking, membranes were incubated with primary antibodies in the blocking solution at 4ºC overnight on shakers. After primary antibody incubation, membranes were washed by TBST (20 mM Tris, pH 7.5, 150 mM NaCl and 0.1% Tween 20). Next, membranes were incubated with secondary antibodies with HRP in the blocking solution at room

temperature for 1 hr. Pierce™ ECL Western Blotting Substrate (ThermoFisher Scientific, 32106) was used for generating chemiluminescent signals.

2.7 DNA qPCR

For short amplicon DNA qPCR, total DNA samples were analyzed by mixing with the primer pairs targeting $tRNA_{Glu}$ (mtDNA) or β-globulin (nDNA) and Luna® Universal qPCR Master Mix (New England Biolabs, M3003S) in the CFX Connect Real-Time PCR Detection System (Bio-Rad Laboratories). The copy number of mtDNA is defined as 2^(Ct of $tRNA_{Glu}$ - Ct of β-globulin).

The long-amplicon qPCR is adapted from Repoles et al., 2021[38]. Total DNA samples or DNA standards were mixed with mtDNA primer pairs (3.4 kb) or nDNA primer pairs (4.5 kb), 200 μM dNTPs, 1x EvaGreen Dye (Biotium, 31000) and 0.63 U PrimeSTAR GXL polymerase (Takara Bio USA, R050A) in the 1x PrimeSTAR GXL buffer. Reactions were performed with the following program: 95℃ for 3 min; 40 cycles of 95℃ for 30 sec and 68℃ for 5 min. mtDNA and nDNA amplicons were defined as the amplification of the long fragment relative to the short fragment, normalizing values to the average of the control groups.

2.8 RT-qPCR

RNA samples were extracted by Quick-RNA™ Miniprep Kit (Zymo Research, R1054) following the manufacturer's instructions. The reverse transcription was

conducted by the high-capacity cDNA reverse transcriptase kit (Applied Biosystems, 4368813).

The cDNAs generated by the high-capacity cDNA reverse transcriptase kit were used for RT-qPCR. The relative quantification method (△△Ct method) was used for gene expression quantification. To obtain △Ct, the Ct of the testing gene was minus the Ct of the house keeping gene glyceraldehyde-3-phosphate dehydrogenase (*GAPDH*) in each sample. Then, the △Ct of the testing gene in each sample was minus the mean △Ct in the control group to get △△Ct. The relative expression level of the testing gene was shown as 2^-△△Ct. The primer used in qPCR was listed in the primer list.

2.9 MitoSOX Staining

Tet-on HeLa cells were cultured on coverslips in 24-well plates 2 days before mt-Ox treatment. After 48 hr of 6 μM mt-Ox or vehicle control treatments, the dosing media were replaced by 500 μL opti-MEM with MitoSOX (5 μM) & DAPI (5 μg/mL) and incubated in the cell incubator for 30 min. After incubation, the cells on coverslips were washed by PBS three times at room temperature. Then, coverslips were transferred to slides and taken images by Leica DMi8 (Leica).

2.10 Statistical Analysis

The data were presented as mean ± standard deviation. Statistical analyses involved Student's t-test and one-way Analysis of Variance (One-way ANOVA)

followed by Tukey's honestly significant difference test with Statistical Product and Service Solutions 27 (IBM). Differences were considered statistically significant at $p < 0.05$.

3 Results

3.1 Mitochondrial Targeting UNG1 Variants Transduced Cell Lines

To understand the cellular responses to different types of mitochondrial DNA lesions, human cell lines (HeLa and HEK293) with inducible mitochondrial targeting uracil DNA glycosylase variants (UNG1-WT, UNG1-Y147A and UNG1-N204D) and APE1 siRNA transfection were used as the mitochondrial AP lesion cell models in this study. Mitochondrial targeting UNG1-Y147A, and UNG1-WT transduced HeLa cell lines were generated in our laboratory previously. In this study, mitochondrial targeting UNG1-N204D transduced HeLa cell lines and three UNG1 variants transduced HEK cell lines were generated.

UNG1-N204D transduced HeLa cell lines expressed MYC-tagged mitochondrial targeting UNG1 only after doxycycline induction; the doxycycline-free samples didn't express the transduced gene (Figure S1A). On the other hand, non-transduced HeLa cells didn't express the transduced gene with the doxycycline treatment (Figure S1A). UNG1 variants transduced HEK293 cell lines also expressed MYC-tagged UNG1 after doxycycline induction (Figure 1B-C and S1B). The results of genotyping indicated both UNG1-Y147A transduced HeLa and HEK 293 cell lines carry the Y147A mutant sequences (Figure 1D). The successfully transduced cells carry the MYC-tagged UNG1 variant sequences in their genomes and express the mitochondrial targeting UNG1 proteins that can be recognized by the anti-MYC antibody.

mtDNA copy number reduction is the signature effect of mitochondrial targeting UNG1 variants overexpression[44]. The copy numbers of mtDNA were significantly reduced in two UNG1-N204D transduced HeLa cell lines after doxycycline induction (Figure S2C-D).

3.2 UNG1 Variant Overexpression and APE1 Knockdown in HeLa Cells

Mitochondrial targeting UNG1 was only expressed in the doxycycline-treated groups, and the mitochondrial APE1 levels were significantly reduced in the APE1-knockdown groups (Figure 2A). The *UNG1* expressions also increased in the doxycycline-treated groups and *APE1* was significantly suppressed in the APE1-knockdown samples (Figure 2E).

mtDNA copy numbers were reduced in doxycycline/non-targeting-siRNA- and doxycycline/APE1-siRNA-treated groups but not altered in APE1-knockedown only group which indicated that the reduction of mtDNA copy was an effect of overexpression of UNG1-Y147A but not of APE1-knockdown (Figure 2B).

To measure the levels of DNA lesions, a qPCR-based method was applied. The mtDNA PCR amplification of APE1-knockedown only group was significantly higher than that in the control, doxycycline/non-targeting-siRNA- and doxycycline/APE1 siRNA-treated groups (Figure 2C). However, the amplification of the non-targeting- siRNA-treated group was slightly induced compared to the control (Figure 2C). siRNA transfection increased the long amplicon PCR amplification of mtDNA, but UNG1 variant overexpression could inhibit the increases in the

cotreatments. On the other hand, the long amplicon PCR amplifications of nDNA were not altered in any treatment (Figure S3A). None of the treatments caused nDNA lesions in HeLa cells.

The expressions of DNA repair genes, *OGG1*, *MUTYH* and *LIG3*, were not altered in any treatment (Figure 2E). Mitochondrial nucleoid gene expressions were not changed in any treatment compared to the control, but the expression of *TFAM* was significantly different between non-targeting-siRNA-treated and doxycycline/APE1-siRNA-treated groups (Figure 2E). Mitochondrial dynamics and mitophagy related genes were not altered in any treatment (Figure 2G and S3B). Neither UNG1-Y147A nor APE1-knockdown significantly affected the gene expressions of mitochondrial nucleoid and mitochondrial dynamics.

The transcripts of mtDNA encoded genes, *ND1* and *ND4*, were significantly reduced in the doxycycline/non-targeting siRNA-treated cells compared to the control cells (Figure 2D). On the other hand, the transcripts in the doxycycline/APE1 siRNA-treated cells were not significantly different from those of the control cells and the transcripts in the APE1-knockdown only cells were slightly increased compared to other groups (Figure 2D). The reduction of mtDNA encoded transcripts in the doxycycline/non-targeting-siRNA-treated cells might be due to the decrease in the mtDNA copy number. The no change of mtDNA encoded transcripts in the doxycycline/APE1-siRNA-treated cells might be due to the counter effect of APE1-knockdown because the transcription of APE1 knockdown only cells were slightly

increased (Figure 2D). The increase of mtDNA transcription efficiency rescued the transcript reduction in the co-treated cells.

3.3 UNG1 Variant Overexpression and APE1 Knockdown in HEK293 Cells

Like the results in the HeLa cells, MYC-tagged mitochondrial targeting UNG1 only expressed in the doxycycline-treated groups and APE1 levels were significantly decreased in the APE1 siRNA treatments (Figure 3A). The mRNA levels of *APE1* and *UNG1* also had the same trends in the APE1-knockdown and doxycycline induced cells, respectively (Figure 3E).

mtDNA copy numbers were also reduced in doxycycline-treated groups (Figure 3B). The mtDNA PCR amplification of APE1 and non-targeting siRNA transfection only groups were significantly increased which indicated the reduction of the PCR-blocking lesions on the mtDNA (Figure 3C). The PCR amplifications of nDNA did not change in any treatment (Figure S4A). The overall trends of mtNDA copy number and PCR amplifications in HEK293 cells were like the trends in the HeLa cells.

Different from the results of HeLa cells, the expression of *TFAM* was not altered and *OGG1* expression increased in the APE1siRNA transfection only group compared to the expression in the control group (Figure 3E-F). Mitochondria fission/fusion related genes (*DRP1* and *MFN1*) and mitophagy related gene (*ATG7*) were significantly induced in the doxycycline/APE1-siRNA-treated group (Figure 3G and S4B).

The transcript levels of mtDNA encoded genes were slightly reduced in the doxycycline/non-targeting-siRNA-treated group compared to the levels in the control group (Figure 3D). *nd4* transcript were significantly increased in the APE1-knockdown only HEK293 cells (Figure 3D).

3.4 HeLa Cells With mt-Ox Treatment

The mitochondrial targeting chemical, mt-Ox, was used to treat human cell lines to generate mtDNA oxidative damage. mt-Ox has an absorbance peak at 500 nm and the absorbance has a good correlation with the concentration of mt-Ox (Figure S5).

The 24 and 48 hr LC_{50} of mt-Ox to HeLa cells were 9.9 and 7.5 μM, respectively (Figure 4A). The NOAECs of cell viability reduction at both 24 and 48 hr were 3 μM, and therefore 3 μM was used as one of the doses in cellular response monitoring experiments.

The cell viabilities of HeLa cells did not change after 8 and 24 hr 3 μM mt-Ox treatment but decreased after 48 hr treatment (Figure 5A). On the other hand, the viabilities of 6 μM mt-Ox-treated HeLa cells for 8, 24 and 48 hr were significantly lower than the viabilities of corresponding vehicle controls (Figure 6A). The signal of mitochondrial superoxide indicator, MitoSOX, was presented in 6 μM mt-Ox-treated HeLa cells but not in the vehicle control cells (Figure S6). Unlike in the UNG1 variant overexpressed cells, the mtDNA copy numbers didn't change in mt-Ox-treated HeLa cells (Figure 5B and 6B). The PCR amplification of the 3.4 kb mtDNA fragment was inhibited by using the total DNA samples from the HeLa cells

with 24 hr 6 μM mt-Ox treatment (Figure 6C), but the amplification of the nDNA fragment was not blocked by using the same DNA samples (Figure S7B). The results indicated that mt-Ox generated PCR-blocking lesions on mtDNA specifically.

The DNA repair related gene, *MUTYH*, was significantly induced in HeLa cells at the 8th hr of 6 μM mt-Ox treatment (Figure 6E). Besides *MUTYH*, the expressions of *APE1*, *UNG1*, *LIG3* but *OGG1* increased after 24 hr of 6 μM mt-Ox treatment (Figure 6E). Whereas only *UNG1* was induced in the 3 μM mt-Ox-treated HeLa cells at the 24th hr (Figure 5E). DNA repair activity seemed higher in the 6 μM mt-Ox-treated HeLa cells. For mitochondrial nucleoid genes, *POLG* was induced but *MGME1* was suppressed in HeLa cells by 8 hr of 6 μM mt-Ox treatment (Figure 6F). The expression of *TFAM* increased at the 24th hr in the 6 μM mt-Ox-treated HeLa cells (Figure 6F). *TWNK* was increased after 24 hr of 3 μM mt-Ox treatment (Figure 5F). Mitochondria fission genes, *DRP1* and *FIS1* were significantly induced in the 6 μM mt-Ox-treated HeLa cells (Figure 6G). On the other hand, the expressions of mitochondria fusion gene, *OPA1*, also increased in the 6 μM mt-Ox-treated HeLa cells at both 8th and 24th hr (Figure 6G). However, *MFN2* transcription only increased at the 24th hr and m*fn1* transcription decreased at the 8th hr (Figure 6G). The transcripts of mtDNA encoded genes, *ND1* and *ND4*, were significantly induced in the 6 μM mt-Ox-treated HeLa cells (Figure 6D). The increase of mtDNA encoded transcripts is a marker of cell stress or cell quality and the ratio of mtDNA encoded transcripts in the RNA samples is used as the threshold for single cell RNA-seq to eliminate low quality cells[26]. Therefore, the increase of mtDNA encoded transcripts

in the 6 μM mt-Ox-treated HeLa cells corresponded to the low cell viability that cells were highly stressed. In summary, DNA repair and mitochondrial dynamics-related genes were significantly induced in the 6 μM mt-Ox-treated HeLa cells that had higher mortalities (Figure 6). On the other hand, the cell responses of 3 μM mt-Ox treatment were mild and had low mortalities and gene alterations (Figure 5).

3.5 HEK Cells With mt-Ox Treatment

The 24 and 48 hr LC_{50} of mt-Ox to HEK293 cells were 18.4 and 18.9 μM, respectively (Figure 4B). The NOAECs of cell viability were 12 and 24 μM at 24 and 48 hr, respectively (Figure 4B). The results showed that HEK293 cells had higher resistance to mt-Ox compared to HeLa cells.

The HEK293 cell viabilities were not altered by 6 μM mt-Ox but slightly reduced after 24 hr of 3 μM mt-Ox treatment (Figure 7A and 8A). The mtDNA copy numbers in HEK293 cells were not altered by mt-Ox (Figure 7B and 8B). Lesions on mtDNA were increased in the HEK293 cells after 48 hr of 6 mt-Ox treatment (Figure 8C), but lesions on nDNA were not induced in the mt-Ox-treated HEK cells (Figure S8A-B).

All tested BER related genes were not altered by 3 or 6 μM mt-Ox (Figure 7E and 8E). *MGME1* expression significantly increased in the 6 μM mt-Ox-treated HEK293 cells at 8^{th} hr but not at 24^{th} and 48^{th} hr (Figure 8F). Mitochondrial fission/fusion and mitophagy gene expressions did not change in the 3 and 6 μM mt-Ox-treated HEK293 cells (Figure 7G, 8G and S8C-D). Mitochondrial DNA encoded

genes showed no change in the mt-Ox-treated HEK293 cells (Figure 7D and 8D). Compared to the HeLa cells, HEK293 cells had weaker gene expression responses to mt-Ox.

4 Discussion

4.1 Overexpression of UNG1 Variant Caused mtDNA Degradation

AP lesion is one of the most abundant DNA lesions in the nucleus[48]. However, the abundance and cellular responses of AP lesions on mtDNA are poorly understood. To address the cellular responses to mitochondrial AP lesions, mitochondrial targeting UNG1 variants overexpression and APE1 siRNA transfection were applied to generate mitochondrial AP lesions in cells. mtDNA copy number reduction was observed in the cells expressing mitochondrial targeting UNG1 variant which has been reported in both animal and cell models previously[22, 23, 44, 54]. mtDNA degradation is a mitochondria specific DNA damage removing process due to the characteristics of multiple copies. mtDNA degradation eliminates highly damaged mtDNA or some detrimental types of mtDNA damage, such as DNA strand breaks[12, 18, 43]. UNG1-Y147A can excise both thymine and uracil on mtDNA creating large amounts of AP sites that might be over the repair capacity[44]. TFAM also converts mitochondrial AP sites into strand breaks which are ready to be removed by mtDNA degradation[59]. Therefore, mtDNA degradation plays an important role in response to UNG1 variant induced mitochondrial AP sites.

The mtDNA encoded transcripts were decreased in the mitochondrial targeting UNG1 variant overexpressing cells. The decreases of mtDNA expression are also detected in other mouse and cell models. The mRNA levels of NADH dehydrogenase 6 (*Nd6*) and cytochrome c oxidase I (*Cox1*) were significantly reduced in the mitochondrial targeting UNG1 variant expressing hippocampus

neurons and cardiomyocytes in mouse[22, 23]. The protein levels of COX1 were also gradually depleted after the mitochondrial targeting UNG1 variants induction in HeLa and 3T3 cells[20, 44]. The reduction of mtDNA transcription might be due to the depletion of mtDNA. If the transcription efficiency was not affected, the reduction of transcription templates (mtDNA) would cause a decrease in the transcripts. The reduction of transcription is an event following the mtDNA degradation.

In this study, the expressions of mitochondria dynamics-related genes were not significantly altered by the induction of the mitochondrial targeting UNG1 variant. However, both mitochondria fission and fusion gene expressions are significantly induced in the mitochondrial targeting UNG1 variant expressing mouse cardiomyocytes[23]. Furthermore, the APE1 signal in the immunostaining of mitochondrial targeting UNG1 variant expressing hippocampus is increased[22]. Whereas the gene expression of *APE1* was not altered in the doxycycline -treated cells in this study. The response difference might be due to the time of induction and different cellular responses in different cell types. The induction time in this study was only 24 hours but the induction times in the mouse studies are 8 weeks or 2 months[22, 23]. The upregulation of mitochondria dynamics-related genes and APE1 might be the chronic responses to the overexpression of mitochondrial targeting UNG1 variant that are not able to be observed in this study.

The overexpression of mitochondrial targeting UNG1 variants also alter mitochondria physiology, such as reducing the oxygen consumption rate (OCR) and mitochondrial membrane potential depolarization[44, 54]. Previous mouse studies also

report that the long-term expression of UNG1 variant causes oxidative stress, induces antioxidative enzymes, such as superoxide dismutase 2 (SOD2), glutathione peroxidase 4 (GPX4) and catalase (CAT), and increases the 8-oxoG signal in the immunostaining images[22, 23]. In contrast, the ROS production is reduced in the HeLa cells after 9-day mitochondrial targeting UNG1 variant induction[45]. ROS is the byproduct of electron transport chain [2], so the reduction of ROS production is due to the ETC activity decease[28]. For the acute responses in the cell cultures, the overexpression of the UNG1 variant generates excessive AP sites inducing mtDNA degradation. The expression of mtDNA encoded ETC subunits is reduced due to the depletion of mtDNA copy. Low expressions of ETC proteins cause ETC activities to be reduced, producing less ROS. On the other hand, in the chronic mouse models, the protein levels of mitochondrial-encoded ETC complexes are also reduced but the level of nuclear-encoded ETC complex II was not affected[22]. The imbalance of ETC complexes might increase the ROS accumulation and inefficient oxidative phosphorylation because the ETC are arranged in a strict order determined by the redox potential of the individual components[22]. The increasing ROS reacts with DNA generating 8-oxoG that activates BER repair in the UNG1 variant expressing cells[22]. The acute and chronic cellular responses to the accumulation of mitochondrial AP lesions might be different due to the sequences of key events.

4.2 mt-Ox Induced Base Excision Repair in HeLa Cells

Accumulation of lipophilic and charged chemicals in the mitochondria and the high amounts of ROS generated by ETC lead mtDNA contains high oxidative lesions[43]. Therefore, understanding the adverse effects and protective pathways of mtDNA oxidative damage are crucial. To investigate the cellular responses to mtDNA oxidative damage, mitochondrial targeting DNA oxidizing agent, mt-Ox, was used to oxidize DNA in mitochondria specifically[57]. The 48 hr LC_{50} of mt-Ox to HeLa cells and HEK293 cells were 7.5 and 18.9 μM, respectively. HEK293 also had higher NOAECs of cell viability reduction than HeLa cells had. HEK293 cells had higher resistance to mt-Ox compared to HeLa cells.

The PCR-blocking lesions were not induced on mtDNA after 8 hr of 6 μM mt-Ox treatments, but after 24 hr in HeLa cells and 48 hr in HEK293 cells. In the previous study, the PCR-blocking lesions are increased on mtDNA but not on nDNA in the cells after 2 hr of 4 μM mt-Ox treatment[57]. The faster lesions formation in the previous work might be due to the additional treatment of DNA samples. 8-oxoG can pair with adenine and cytosine, so it can be bypass during DNA synthesis. It is not a strong PCR-blocking lesion[31]. In the previous study, DNA samples are treated with fapy glycosylase (FPG) that creates single strand breaks at the sites of 8-oxoG to convert 8-oxoG into PCR-blocking lesions[57]. Therefore, both 8-oxoG and other PCR-blocking lesions, such as SSB and DSB, can be detected in the previous study. In contrast, only endogenous PCR-blocking lesions were detected in this study.

DNA repair genes, *APE1*, *UNG1*, *MUTYH* and *LIG3*, were significantly induced in the 6 μM mt-Ox-treated HeLa cells at the 24th hr. *MUTYH* was also upregulated in the 8th hr after light activation. In the previous study, authors combine DNA repair siRNA knockdown array and mt-Ox treatment to screen the important genes for mtDNA repair. The knockdown of *APE1*, *MUTYH*, and *LIG3* significantly increase the mt-Ox toxicity in MRC-5 cells. In contrast, the *OGG1* and *UNG1* knockdown do not induce the mt-Ox toxicity in the screening[57]. Both studies agree that *APE1*, *MUTYH* and *LIG3* participate in the response to mt-Ox induced toxicity. Therefore, DNA repair might play an important role in removing mtDNA oxidative damage.

Except treating mitochondrial targeting DNA oxidizing agent, depletions of DNA oxidative damage removing glycosylases, such as OGG1 and MUTYH, are applied to increase mtDNA oxidative damage. For example, *Ogg1*-knockout mice are analyzed for mtDNA alteration. Interestingly, mtDNA content is increased in the *Ogg1*-knockout mice compared to the content in the wild type mice. FPG sensitive sites on mtDNA also elevate in the *Ogg1*-knockout mice and the D-loop region is most severely affected by the absence of OGG1[6]. To prevent the increase of nDNA oxidative damage, Kauppila *et al*. only exclude OGG1 from mitochondria by removing the mitochondrial targeting sequence of *Ogg1* in the mice[16]. The mtDNA copy number was slightly increased in the liver of *Ogg1* MTS deleted mice, but the mtDNA mutation rate is not increased[16]. In the same study, heart *Sod2*-knockout mice had no decrease in mtDNA copy number with high oxidative stress. The mutation rate is not induced in *Sod*- knockout or *Sod2*-knockout x *Ogg1* MTS

deleted mice either[16]. These results indicate that the depletion of OGG1 can induce mtDNA oxidative damage and increase the mtDNA copy number in mice. The reason for mtDNA copy number increase might be due to the increase of mtDNA synthesis in the OGG1 depleted mice[6].

Previous studies show that the accumulation of mtDNA lesions and mtDNA copy number reduction can simultaneously exist in the cells under oxidative stress. In addition, mtDNA repair and mtDNA degradation are competitive pathways to eliminate mtDNA damage. For example, both H_2O_2 and xanthine oxidase increase the mtDNA strand breaks and reduce mtDNA copy numbers in HCT116 cells[43]. The additional treatment of BER inhibitor methoxyamine further decreases the mtDNA contents which indicates the enhancement of mtDNA degradation[43]. In this study, mtDNA lesions but mtDNA copy number reduction were detected in the mt-Ox-treated cells. The possible reason that mtDNA degradation was absent in mt-Ox-treated HeLa cells might be due to the levels of mtDNA damage. The intact mtDNA levels are less than 20% compared to the control in the xanthine-oxidase-treated cells[43], but the mtDNA relative amplicons of mt-Ox-treated cells were above 30% (Figure 6C). DNA repair related genes were also upregulated to repair the mtDNA (Figure 6E). DNA repair might be sufficient to eliminate the mtDNA damage in the mt-Ox-treated cells, but not enough to repair the damage in the xanthine-oxidase-treated cells. To validate this hypothesis, the cotreatment of BER inhibitors and mt-Ox or increasing mt-Ox concentration are considered.

4.3 Cellular Responses in Two mtDNA Lesion Models Are Different

In the mtDNA AP lesion cell models, mtDNA copy numbers were significantly reduced but PCR-blocking lesions did not increase on mtDNA. The transcripts of mt-DNA encoded genes were also reduced due to the decreases of transcription templates. However, DNA repair, mitochondrial nucleoid and mitochondria dynamics-related genes were not significantly altered in the AP lesion models. On the other hand, in the mtDNA oxidative damage cell models, mtDNA copy numbers didn't change but the PCR-blocking lesions on mtDNA increased. The expressions of mtDNA encoded genes, DNA repair and mitochondria dynamics-related genes were increased in the mt-Ox-treated HeLa cells. The cellular responses in the two mtDNA damage cell models were different which indicated cells might have different damage responses to variable types of mtDNA damage or the degree of damage. Previous studies already show that the mtDNA degradation activity is positively correlated to the mtDNA oxidative damage level, and mtDNA alkylating damage is unlikely to induce mtDNA degradation[43]. While mtDNA DSBs are prone to induce mtDNA degradation rather than DNA repair[12]. The contributions of mtDNA damage elimination pathways are dependent on both types and the extent of damage.

DNA oxidative damage, such as 8-oxoG, can be repaired by BER and AP site is an intermediate in the BER process[18]. BER related genes were also induced in the 6 μM mt-Ox-treated HeLa cells. As the intermediates, mitochondrial AP sites might also increase in the mt-Ox-treated HeLa cells, but mtDNA copy number did not

decrease like in the mitochondrial targeting UNG1 variant expressing HeLa cells. The reason might be due to the increase of mtDNA synthesis because the gene expression of mtDNA polymerase *POLG* and mtDNA nucleoid protein *TFAM* were induced. Furthermore, the upregulation of DNA repair which competes with mtDNA degradation also prevents the mtDNA degrdation[43]. In contrast, the expressions of downstream BER genes, *APE1* and *LIG3*, were not induced in the AP lesion models. Mitochondrial BER might be only activated by the substrates of DNA glycosylases which start the BER processes. Therefore, both oxidative and alkylating lesions can be well repaired within the repair capacity[43]. As an intermediate of BER, AP site is not able to activate BER in mitochondria. Without sufficient DNA repair, mtDNA degradation is dominated to eliminate DNA lesions in mitochondria.

The changes of mtDNA encoded gene expressions were opposite in two mtDNA damage cell models. The expressions were suppressed in the AP lesion models, but the expressions were increased in the oxidative damage models. The opposite response is due to the causes being different. The reduction in AP lesion models is due to the depletion of mtNDA copies, whereas the induction in the oxidative damage models is due to the cell death that is absent in the mt-Ox-treated cells with low mortalities. The induction of mitochondria fission and fusion in the 6 μM mt-Ox-treated HeLa cells might be due to the same reason. Previous study shows that mitochondrial toxin acrolein also induces the expression of mitochondria fission proteins with the activation of apoptosis and elevation of mitochondrial ROS[53]. The

induction of mitochondria fission and fusion might be an indirect response to the mtDNA oxidative damage in the 6 μM mt-Ox-treated HeLa cells.

4.4 Future Directions

In this study, significantly different cellular responses in the different mtDNA damage cell models were revealed, but the reasons underlying the response differences are unclear. The differences are due to the levels of damage, the types of damage or other reasons are still questionable. To validate whether cells have different responses to different levels of mtDNA damage, a reliable mtDNA damage quantification method is essential. Although the qPCR-based method was already applied in this study, it still has some limitations. For example, some types of lesions, such as AP sites and 8-oxoG, are not PCR-blocking lesions that can't be detected by qPCR[31]. Additional enzyme treatments, such as FPG or APE1, converting bypassed lesions into SSBs which can block PCR reactions might be helpful to overcome this limitation[31]. The qPCR-based method is a relative quantification method, so it is hard to compare the results between different batches of experiment. Hence, an absolute quantification is required for comparing the results from different experiments or lesions. Mass spectrometry is an alternative method for quantifying mtDNA lesions. Many reliable methods to measure different types of DNA lesions in biological samples by mass spectrometry have been developed[51]. However, there are some problems that mass-spectrum-based methods should overcome. For example, the purity of mtDNA samples must be high because the mass spectrum cannot

differentiate mtDNA and nDNA. The contamination of nDNA is a big problem. Therefore, a good sample preparation process is essential for the mass spectrum. Whereas total DNA can be used in qPCR-based methods by using mtDNA specific primers. In conclusion, a reliable method to quantify the absolute number of mtDNA lesions is necessary for comparing different mtDNA damage models.

Although mt-Ox is a well-designed chemical for targeting mitochondria, it might cause other oxidative damage, such as lipid peroxidation and protein oxidation[14]. The cellular responses might be due to the off-target effects. Therefore, the cell death, mitochondrial dynamics alteration and the increase of mtDNA encoded transcripts might be due to the oxidative damage of other biomolecules in the cells (Figure 6). It is difficult to generate mtDNA oxidative damage without causing other side effects. Chemicals might react with other biomolecules. Knockout and knockdown of DNA repair genes might have compensated or off-target effects in cells. A novel and precise tool to generate mtDNA oxidative damage in cells is expected.

The damage recognition and damage responses initiation processes are unclear but important for the damage response regulations. Therefore, the mechanisms of damage recognition and damage response initiation are also worth investigating. The linkages and the sequences of mtDNA damage are also required to depict the mtDNA damage induced adverse outcome pathways. As previously mentioned, the sequences of mtDNA AP lesions induced acute effects are relatively clear. However, the sequences and mechanisms of chronic effects are unclear. Hence, mapping the adverse effects is also important. Besides AP sites and oxidative damage, other types

of DNA damage, such as alkylation, mismatch, and DNA strand breaks, were also presented on mtDNA[63]. Investigating the cellular responses of other types of mtDNA damage at different levels is also important. Different cell types, such as primary cell cultures or induced pluripotent stem cells, should be tested to confirm the cellular responses observed in the mtDNA damage human cell line models are universal in human cells. The further validations in animal models can provide more information about the adverse effects in the higher levels. Overall, mtDNA is a vulnerable and significant target for environmental stress, so understanding mtNDA induced cellular responses and adverse effects is important for protecting human and environmental health.

5 Conclusion

This study shows that human cell lines had different responses to mtDNA AP sites and oxidative damage. Overexpression of mitochondrial targeting UNG1 variants generated mtDNA specific AP lesions and decreased the mtDNA copy number in both HeLa and HEK293 cells. The transcripts of mtDNA encoded genes were decreased due to the reduction of transcription templates. Whereas DNA repair and mitochondria dynamics-related genes were not significantly altered. mtDNA degradation was the main response in the mtDNA AP lesion cell models. On the other hand, mt-Ox caused PCR-blocking lesions on mtDNA exclusively without inducing mtDNA degradation. DNA repair and mitochondria dynamics-related genes were upregulated in mt-Ox-treated HeLa cells. DNA repair was more significant in the mtDNA oxidative damage models. Overall, this study provides insights into different cellular responses to two types of mtDNA lesions and guides future research in investigating factors involved in processing these lesions.

6 Reference

1. Barker, S.; Weinfeld, M.; Murray, D., DNA-protein crosslinks: their induction, repair, and biological consequences. *Mutat. Res. - Rev. Mut. Res.* **2005,** *589*, (2), 111-135.

2. Berghmans, S.; Murphey, R. D.; Wienholds, E.; Neuberg, D.; Kutok, J. L.; Fletcher, C. D.; Morris, J. P.; Liu, T. X.; Schulte-Merker, S.; Kanki, J. P.; Plasterk, R.; Zon, L. I.; Look, A. T., tp53 mutant zebrafish develop malignant peripheral nerve sheath tumors. *Proc Natl Acad Sci U S A* **2005,** *102*, (2), 407-12.

3. Bess, A. S.; Crocker, T. L.; Ryde, I. T.; Meyer, J. N., Mitochondrial dynamics and autophagy aid in removal of persistent mitochondrial DNA damage in Caenorhabditis elegans. *Nucleic Acids Res.* **2012,** *40*, (16), 7916-31.

4. Chamberlain, G. R.; Tulumello, D. V.; Kelley, S. O., Targeted delivery of doxorubicin to mitochondria. *ACS Chem Biol* **2013,** *8*, (7), 1389-95.

5. Chandra, R.; Engeln, M.; Schiefer, C.; Patton, M. H.; Martin, J. A.; Werner, C. T.; Riggs, L. M.; Francis, T. C.; McGlincy, M.; Evans, B.; Nam, H.; Das, S.; Girven, K.; Konkalmatt, P.; Gancarz, A. M.; Golden, S. A.; Iniguez, S. D.; Russo, S. J.; Turecki, G.; Mathur, B. N.; Creed, M.; Dietz, D. M.; Lobo, M. K., Drp1 Mitochondrial Fission in D1 Neurons Mediates Behavioral and Cellular Plasticity during Early Cocaine Abstinence. *Neuron* **2017,** *96*, (6), 1327-1341 e6.

6. Chimienti, G.; Pesce, V.; Fracasso, F.; Russo, F.; de Souza-Pinto, N. C.; Bohr, V. A.; Lezza, A. M. S., Deletion of OGG1 Results in a Differential Signature of Oxidized Purine Base Damage in mtDNA Regions. *International journal of molecular sciences* **2019,** *20*, (13).

7. Cooke, M. S.; Evans, M. D.; Dizdaroglu, M.; Lunec, J., Oxidative DNA damage: mechanisms, mutation, and disease. *FASEB J.* **2003,** *17*, (10), 1195-214.

8. Dreier, D. A.; Mello, D. F.; Meyer, J. N.; Martyniuk, C. J., Linking Mitochondrial Dysfunction to Organismal and Population Health in the Context of Environmental Pollutants: Progress and Considerations for Mitochondrial Adverse Outcome Pathways. *Environ Toxicol Chem* **2019,** *38*, (8), 1625-1634.

9. Fan, W. W.; Waymire, K. G.; Narula, N.; Li, P.; Rocher, C.; Coskun, P. E.; Vannan, M. A.; Narula, J.; MacGregor, G. R.; Wallace, D. C., A mouse model of mitochondrial disease reveals germline selection against severe mtDNA mutations. *Science* **2008,** *319*, (5865), 958-962.

10. Fonseca, S. B.; Pereira, M. P.; Mourtada, R.; Gronda, M.; Horton, K. L.; Hurren, R.; Minden, M. D.; Schimmer, A. D.; Kelley, S. O., Rerouting chlorambucil to mitochondria combats drug deactivation and resistance in cancer cells. *Chem. Biol.* **2011,** *18*, (4), 445-53.

11. Fontana, G. A.; Gahlon, H. L., Mechanisms of replication and repair in mitochondrial DNA deletion formation. *Nucleic Acids Res.* **2020,** *48*, (20), 11244-11258.

12. Fu, Y.; Tigano, M.; Sfeir, A., Safeguarding mitochondrial genomes in higher eukaryotes. *Nat. Struct. Mol. Biol.* **2020,** *27*, (8), 687-695.

13. Gonzalez-Hunt, C. P.; Rooney, J. P.; Ryde, I. T.; Anbalagan, C.; Joglekar, R.; Meyer, J. N., PCR-Based Analysis of Mitochondrial DNA Copy Number, Mitochondrial DNA Damage, and Nuclear DNA Damage. *Curr Protoc Toxicol* **2016,** *67*, 20 11 1-20 11 25.

14. Gorrini, C.; Harris, I. S.; Mak, T. W., Modulation of oxidative stress as an anticancer strategy. *Nature Reviews Drug Discovery* **2013,** *12*, (12), 931-947.

15. Ikeda, S.; Ozaki, K., Action of mitochondrial endonuclease G on DNA damaged by L-ascorbic acid, peplomycin, and cis-diamminedichloroplatinum (II). *Biochem. Biophys. Res. Commun.* **1997,** *235*, (2), 291-294.

16. Kauppila, J. H. K.; Bonekamp, N. A.; Mourier, A.; Isokallio, M. A.; Just, A.; Kauppila, T. E. S.; Stewart, J. B.; Larsson, N. G., Base-excision repair deficiency alone or combined with increased oxidative stress does not increase mtDNA point mutations in mice. *Nucleic Acids Res.* **2018,** *46*, (13), 6642-6669.

17. Kavli, B.; Slupphaug, G.; Mol, C. D.; Arvai, A. S.; Petersen, S. B.; Tainer, J. A.; Krokan, H. E., Excision of cytosine and thymine from DNA by mutants of human uracil-DNA glycosylase. *EMBO J.* **1996,** *15*, (13), 3442-3447.

18. Kazak, L.; Reyes, A.; Holt, I. J., Minimizing the damage: repair pathways keep mitochondrial DNA intact. *Nature reviews. Molecular cell biology* **2012,** *13*, (10), 659-71.

19. Kim, D. V.; Kulishova, L. M.; Torgasheva, N. A.; Melentyev, V. S.; Dianov, G. L.; Medvedev, S. P.; Zakian, S. M.; Zharkov, D. O., Mild phenotype of knockouts of the major apurinic/apyrimidinic endonuclease APEX1 in a non-cancer human cell line. *PloS one* **2021,** *16*, (9), e0257473.

20. Kozhukhar, N.; Spadafora, D.; Fayzulin, R.; Shokolenko, I. N.; Alexeyev, M., The efficiency of the translesion synthesis across abasic sites by mitochondrial DNA polymerase is low in mitochondria of 3T3 cells. *Mitochondrial DNA A* **2016,** *27*, (6), 4390-4396.

21. Larsson, N. G.; Wang, J. M.; Wilhelmsson, H.; Oldfors, A.; Rustin, P.; Lewandoski, M.; Barsh, G. S.; Clayton, D. A., Mitochondrial transcription factor A is necessary for mtDNA maintenance and embryogenesis in mice. *Nat. Genet.* **1998,** *18*, (3), 231-236.

22. Lauritzen, K. H.; Cheng, C.; Wiksen, H.; Bergersen, L. H.; Klungland, A., Mitochondrial DNA toxicity compromises mitochondrial dynamics and induces hippocampal antioxidant defenses. *DNA Repair (Amst)* **2011,** *10*, (6), 639-53.

23. Lauritzen, K. H.; Kleppa, L.; Aronsen, J. M.; Eide, L.; Carlsen, H.; Haugen, O. P.; Sjaastad, I.; Klungland, A.; Rasmussen, L. J.; Attramadal, H.; Storm-Mathisen, J.; Bergersen, L. H., Impaired dynamics and function of mitochondria caused by mtDNA toxicity leads to heart failure. *Am. J. Physiol. Heart Circ. Physiol.* **2015,** *309*, (3), H434-49.

24. Lieber, T.; Jeedigunta, S. P.; Palozzi, J. M.; Lehmann, R.; Hurd, T. R., Mitochondrial fragmentation drives selective removal of deleterious mtDNA in the germline. *Nature* **2019,** *570*, (7761), 380-+.

25. Liu, Y. J.; McIntyre, R. L.; Janssens, G. E.; Houtkooper, R. H., Mitochondrial fission and fusion: A dynamic role in aging and potential target for age-related disease. *Mech Ageing Dev* **2020,** *186*, 111212.

26. Luecken, M. D.; Theis, F. J., Current best practices in single-cell RNA-seq analysis: a tutorial. *Mol. Syst. Biol.* **2019,** *15*, (6), e8746.

27. Luz, A. L.; Godebo, T. R.; Bhatt, D. P.; Ilkayeva, O. R.; Maurer, L. L.; Hirschey, M. D.; Meyer, J. N., From the Cover: Arsenite Uncouples Mitochondrial Respiration and Induces a Warburg-like Effect in Caenorhabditis elegans. *Toxicological sciences : an official journal of the Society of Toxicology* **2016,** *152*, (2), 349-62.

28. Meyer, J. N.; Hartman, J. H.; Mello, D. F., Mitochondrial Toxicity. *Toxicological sciences : an official journal of the Society of Toxicology* **2018,** *162*, (1), 15-23.

29. Nicholls, T. J.; Zsurka, G.; Peeva, V.; Scholer, S.; Szczesny, R. J.; Cysewski, D.; Reyes, A.; Kornblum, C.; Sciacco, M.; Moggio, M.; Dziembowski, A.; Kunz, W. S.; Minczuk, M., Linear mtDNA fragments and unusual mtDNA rearrangements associated with pathological deficiency of MGME1 exonuclease. *Hum. Mol. Genet.* **2014,** *23*, (23), 6147-62.

30. Nissanka, N.; Bacman, S. R.; Plastini, M. J.; Moraes, C. T., The mitochondrial DNA polymerase gamma degrades linear DNA fragments precluding the formation of deletions. *Nat Commun* **2018,** *9*, (1), 2491.

31. O'Callaghan, N.; Baack, N.; Sharif, R.; Fenech, M., A qPCR-based assay to quantify oxidized guanine and other FPG-sensitive base lesions within telomeric DNA. *BioTechniques* **2011,** *51*, (6), 403-11.

32. Otten, A. B. C.; Kamps, R.; Lindsey, P.; Gerards, M.; Pendeville-Samain, H.; Muller, M.; van Tienen, F. H. J.; Smeets, H. J. M., Tfam Knockdown Results in Reduction of mtDNA Copy Number, OXPHOS Deficiency and Abnormalities in Zebrafish Embryos. *Front Cell Dev Biol* **2020,** *8*, 381.

33. Paes Dias, M.; Tripathi, V.; van der Heijden, I.; Cong, K.; Manolika, E. M.; Bhin, J.; Gogola, E.; Galanos, P.; Annunziato, S.; Lieftink, C.; Andujar-Sanchez, M.; Chakrabarty, S.; Smith, G. C. M.; van de Ven, M.; Beijersbergen, R. L.; Bartkova, J.; Rottenberg, S.; Cantor, S.; Bartek, J.; Ray Chaudhuri, A.; Jonkers, J., Loss of nuclear DNA ligase III reverts PARP inhibitor resistance in BRCA1/53BP1 double-deficient cells by exposing ssDNA gaps. *Mol. Cell* **2021,** *81*, (22), 4692-4708 e9.

34. Peeva, V.; Blei, D.; Trombly, G.; Corsi, S.; Szukszto, M. J.; Rebelo-Guiomar, P.; Gammage, P. A.; Kudin, A. P.; Becker, C.; Altmuller, J.; Minczuk, M.; Zsurka, G.; Kunz, W. S., Linear mitochondrial DNA is rapidly degraded by components of the replication machinery. *Nat Commun* **2018,** *9*, (1), 1727.

35. Pfanner, N.; Warscheid, B.; Wiedemann, N., Mitochondrial proteins: from biogenesis to functional networks. *Nature reviews. Molecular cell biology* **2019,** *20*, (5), 267-284.

36. Qian, W.; Kumar, N.; Roginskaya, V.; Fouquerel, E.; Opresko, P. L.; Shiva, S.; Watkins, S. C.; Kolodieznyi, D.; Bruchez, M. P.; Van Houten, B., Chemoptogenetic damage to mitochondria causes rapid telomere dysfunction. *P Natl Acad Sci USA* **2019,** *116*, (37), 18435-18444.

37. Quinones, J. L.; Thapar, U.; Wilson, S. H.; Ramsden, D. A.; Demple, B., Oxidative DNA-protein crosslinks formed in mammalian cells by abasic site lyases involved in DNA repair. *DNA Repair (Amst)* **2020,** *87*, 102773.

38. Repoles, B. M.; Gorospe, C. M.; Tran, P.; Nilsson, A. K.; Wanrooij, P. H., The integrity and assay performance of tissue mitochondrial DNA is considerably affected by choice of isolation method. *Mitochondrion* **2021,** *61*, 179-187.

39. Robb, E. L.; Gawel, J. M.; Aksentijevic, D.; Cocheme, H. M.; Stewart, T. S.; Shchepinova, M. M.; Qiang, H.; Prime, T. A.; Bright, T. P.; James, A. M.; Shattock, M. J.; Senn, H. M.; Hartley, R. C.; Murphy, M. P., Selective superoxide generation within mitochondria by the targeted redox cycler MitoParaquat. *Free Radical Biol. Med.* **2015,** *89*, 883-894.

40. Roubicek, D. A.; de Souza-Pinto, N. C., Mitochondria and mitochondrial DNA as relevant targets for environmental contaminants. *Toxicology* **2017,** *391*, 100-108.

41. Sanders, L. H.; Howlett, E. H.; McCoy, J.; Greenamyre, J. T., Mitochondrial DNA damage as a peripheral biomarker for mitochondrial toxin exposure in rats. *Toxicological sciences : an official journal of the Society of Toxicology* **2014,** *142*, (2), 395-402.

42. Scholz, S.; Nichols, J. W.; Escher, B. I.; Ankley, G. T.; Altenburger, R.; Blackwell, B.; Brack, W.; Burkhard, L.; Collette, T. W.; Doering, J. A.; Ekman, D.; Fay, K.; Fischer, F.; Hackermuller, J.; Hoffman, J. C.; Lai, C.; Leuthold, D.; Martinovic-Weigelt, D.; Reemtsma, T.; Pollesch, N.; Schroeder, A.; Schuurmann, G.; von Bergen, M., The Eco-Exposome Concept: Supporting an Integrated Assessment of Mixtures of Environmental Chemicals. *Environ Toxicol Chem* **2022,** *41*, (1), 30-45.

43. Shokolenko, I.; Venediktova, N.; Bochkareva, A.; Wilson, G. L.; Alexeyev, M. F., Oxidative stress induces degradation of mitochondrial DNA. *Nucleic Acids Res.* **2009,** *37*, (8), 2539-48.

44. Shokolenko, I. N.; Wilson, G. L.; Alexeyev, M. F., Persistent damage induces mitochondrial DNA degradation. *DNA Repair (Amst)* **2013,** *12*, (7), 488-99.

45. Spadafora, D.; Kozhukhar, N.; Chouljenko, V. N.; Kousoulas, K. G.; Alexeyev, M. F., Methods for Efficient Elimination of Mitochondrial DNA from Cultured Cells. *PloS one* **2016,** *11*, (5), e0154684.

46. St John, J. C., Mitochondria and Female Germline Stem Cells-A Mitochondrial DNA Perspective. *Cells-Basel* **2019,** *8*, (8).

47. Stewart, J. B.; Chinnery, P. F., The dynamics of mitochondrial DNA heteroplasmy: implications for human health and disease. *Nat Rev Genet* **2015,** *16*, (9), 530-42.

48. Swenberg, J. A.; Lu, K.; Moeller, B. C.; Gao, L.; Upton, P. B.; Nakamura, J.; Starr, T. B., Endogenous versus exogenous DNA adducts: their role in carcinogenesis, epidemiology, and risk assessment. *Toxicological sciences : an official journal of the Society of Toxicology* **2011,** *120 Suppl 1*, S130-45.

49. Szczesny, B.; Marcatti, M.; Ahmad, A.; Montalbano, M.; Brunyanszki, A.; Bibli, S. I.; Papapetropoulos, A.; Szabo, C., Mitochondrial DNA damage and subsequent activation of Z-DNA binding protein 1 links oxidative stress to inflammation in epithelial cells. *Sci Rep* **2018,** *8*, (1), 914.

50. Tigano, M.; Vargas, D. C.; Tremblay-Belzile, S.; Fu, Y.; Sfeir, A., Nuclear sensing of breaks in mitochondrial DNA enhances immune surveillance. *Nature* **2021,** *591*, (7850), 477-481.

51. Tretyakova, N.; Villalta, P. W.; Kotapati, S., Mass spectrometry of structurally modified DNA. *Chem. Rev.* **2013,** *113*, (4), 2395-436.

52. Van Houten, B.; Hunter, S. E.; Meyer, J. N., Mitochondrial DNA damage induced autophagy, cell death, and disease. *Front Biosci-Landmrk* **2016,** *21*, 42-54.

53. Wang, H. T.; Lin, J. H.; Yang, C. H.; Haung, C. H.; Weng, C. W.; Lin, A. M. Y.; Lo, Y. L.; Chen, W. S.; Tang, M. S., Acrolein induces mtDNA damages, mitochondrial fission and mitophagy in human lung cells. *Oncotarget* **2017,** *8*, (41), 70406-70421.

54. Wang, Y.; Wang, X.; Long, Q.; Liu, Y.; Yin, T.; Sirota, I.; Ren, F.; Gu, Z.; Luo, J., Reducing embryonic mtDNA copy number alters epigenetic profile of key hepatic lipolytic genes and causes abnormal lipid accumulation in adult mice. *FEBS J.* **2021**.

55. Weatherly, L. M.; Nelson, A. J.; Shim, J.; Riitano, A. M.; Gerson, E. D.; Hart, A. J.; de Juan-Sanz, J.; Ryan, T. A.; Sher, R.; Hess, S. T.; Gosse, J. A., Antimicrobial agent triclosan disrupts mitochondrial structure, revealed by super-resolution microscopy, and inhibits mast cell signaling via calcium modulation. *Toxicology and applied pharmacology* **2018,** *349*, 39-54.

56. West, A. P.; Shadel, G. S., Mitochondrial DNA in innate immune responses and inflammatory pathology. *Nat Rev Immunol* **2017,** *17*, (6), 363-375.

57. Wisnovsky, S.; Jean, S. R.; Kelley, S. O., Mitochondrial DNA repair and replication proteins revealed by targeted chemical probes. *Nat. Chem. Biol.* **2016,** *12*, (7), 567-73.

58. Xian, H.; Watari, K.; Sanchez-Lopez, E.; Offenberger, J.; Onyuru, J.; Sampath, H.; Ying, W.; Hoffman, H. M.; Shadel, G. S.; Karin, M., Oxidized DNA fragments exit mitochondria via mPTP- and VDAC-dependent channels to activate NLRP3 inflammasome and interferon signaling. *Immunity* **2022**.

59. Xu, W. Y.; Boyd, R. M.; Tree, M. O.; Samkari, F.; Zhao, L. L., Mitochondrial transcription factor A promotes DNA strand cleavage at abasic sites. *P Natl Acad Sci USA* **2019,** *116*, (36), 17792-17799.

60. Yan, C.; Duanmu, X.; Zeng, L.; Liu, B.; Song, Z., Mitochondrial DNA: Distribution, Mutations, and Elimination. *Cells-Basel* **2019,** *8*, (4).

61. Zhang, R.; Wang, J., HuR stabilizes TFAM mRNA in an ATM/p38-dependent manner in ionizing irradiated cancer cells. *Cancer Sci.* **2018,** *109*, (8), 2446-2457.

62. Zhang, Y.; Yao, Y.; Qiu, X.; Wang, G.; Hu, Z.; Chen, S.; Wu, Z.; Yuan, N.; Gao, H.; Wang, J.; Song, H.; Girardin, S. E.; Qian, Y., Listeria hijacks host mitophagy through a novel mitophagy receptor to evade killing. *Nat. Immunol.* **2019,** *20*, (4), 433-446.

63. Zhao, L.; Sumberaz, P., Mitochondrial DNA Damage: Prevalence, Biological Consequence, and Emerging Pathways. *Chemical research in toxicology* **2020,** *33*, (10), 2491-2502.

64. Zolkipli-Cunningham, Z.; Falk, M. J., Clinical effects of chemical exposures on mitochondrial function. *Toxicology* **2017,** *391*, 90-99.

Tables

Table 1. Primer list.

Name	Purpose	Sequence		Reference
mt-ung1	Genotyping	F	ATGCTGTTTAATCTGAGGAT	This study
		R	TCACAGCTCCTTCCAGTCAA	
8.9 kb mtDNA	qPCR standard	F	TCTAAGCCTCCTTATTCGAGCCGA	13
		R	TTTCATCATGCGGAGATGTTGGATGG	
13.5 kb nDNA	qPCR standard	F	GCACTGGCTTAGGAGTTGGACT	13
		R	CGAGTAAGAGACCATTGTGGCAG	
3.4 kb mtDNA	DNA qPCR	F	TAAAGCCCATGTCGAAGCCC	This study
		R	TTTCATCATGCGGAGATGTTGGATGG	
4.5 kb nDNA	DNA qPCR	F	AGGTGGTGGCATGGTTTGAT	This study
		R	CGAGTAAGAGACCATTGTGGCAG	
$tRNA_{Glu}$	DNA qPCR	F	CCCCACAAACCCCATTACTAAACCCA	This study
		R	TTTCATCATGCGGAGATGTTGGATGG	
BGLO	DNA qPCR	F	AGGGTCTTGGGTACAGGAGTT	This study
		R	CGAGTAAGAGACCATTGTGGCAG	
GAPDH	RT qPCR	F	GAGAGAGACCCTCACTGCTG	5
		R	TCCCCTCTTCAAGGGGTCTA	
DRP1	RT qPCR	F	CAAAGCAGTTTGCCTGTGGA	5
		R	TCTTGGAGGACTATGGCAGC	
FIS1	RT qPCR	F	CCAAATCCTGAAGGAGACGC	5
		R	GCTGAAGGCCACAGAGGATA	
OPA1	RT qPCR	F	ACGTCTTTTGTCCAGCCTCT	5
		R	GGTTAAAGCGCCCGTAACAT	
MFN1	RT qPCR	F	CCTGGCATCCAGGAGTTAGA	5
		R	TGGTTCCAGCAATGCGATTT	
MFN2	RT qPCR	F	TGCAGGTGTAAGGGACGATT	5
		R	GAGGCTCTGCAAATGGGATG	
PINK1	RT qPCR	F	CTGTCAGGAGATCCAGGCAATT	62
		R	GCATGGTGGCTTCATACACAGC	
ATG7	RT qPCR	F	CTGCCAGCTCGCTTAACATTG	62
		R	CTTGTTGAGGAGTACAGGGTTTT	
APE1	RT qPCR	F	GTTTCTTACGGCATAGGCGAT	19
		R	CACAAACGAGTCAAATTCAGCC	

Name	Purpose	Sequence		Reference
OGG1	RT qPCR	F	ACTCCCACTTCCAAGAGGTG	19
		R	GGATGAGCCGAGGTCCAAAAG	
UNG1	RT qPCR	F	CCCCACACCAAGTCTTCACC	19
		R	TTGAACACTAAAGCAGAGCCC	
MUTYH	RT qPCR	F	ATACCGGATGGATGCAGAAGT	19
		R	GCCCAGAGTTGATTCACCTCC	
LIG3	RT qPCR	F	GCCGGAGAGGCAGCTATATG	33
		R	GGCAACAGTTCTTTTCGGCTG	
MGME1	RT qPCR	F	ACAGCGGATGATTCTGGAAC	34
		R	TCGCACTCCACTGACATCTT	
ENDOG	RT qPCR	F	GGACGACACGTTCTACCTGA	34
		R	CCTGTGCAGACATAGACGTT	
TWNK	RT qPCR	F	GGCTGGAAGATCAACTGGACAA	34
		R	ACTGCAGGTTGTCGATGATCAC	
POLG	RT qPCR	F	TGGCAGGAGCAGTTAGTGGT	34
		R	TGCTATCCACAGACTGCGCT	
TFAM	RT qPCR	F	GCGCTCCCCCTTCAGTTTTG	61
		R	GTTTTTGCATCTGGGTTCTGAGC	
ND1	RT qPCR	F	AGGCCTCCTATTTATTCTAGCCAC	This study
		R	CGGCTATGAAGAATAGGGCGA	
ND4	RT qPCR	F	TAAAGCCCATGTCGAAGCCC	This study
		R	CGAGGGCTATGTGGCTGATT	
ND5	RT qPCR	F	AACTGTTCATCGGCTGAGAGG	This study
		R	GTCAGGGGTGGAGACCTAATTG	

Table 2. Antibodies used in the thesis.

Antibody	Company	Catalog No.	Host	Ab Type
TOM20	Cell Signaling	42406	Rabbit	mAb
APE1	Santa Cruz	sc-55498	Mouse	mAb
c-Myc Tag	Genscript	A00704	Mouse	mAb

Figures

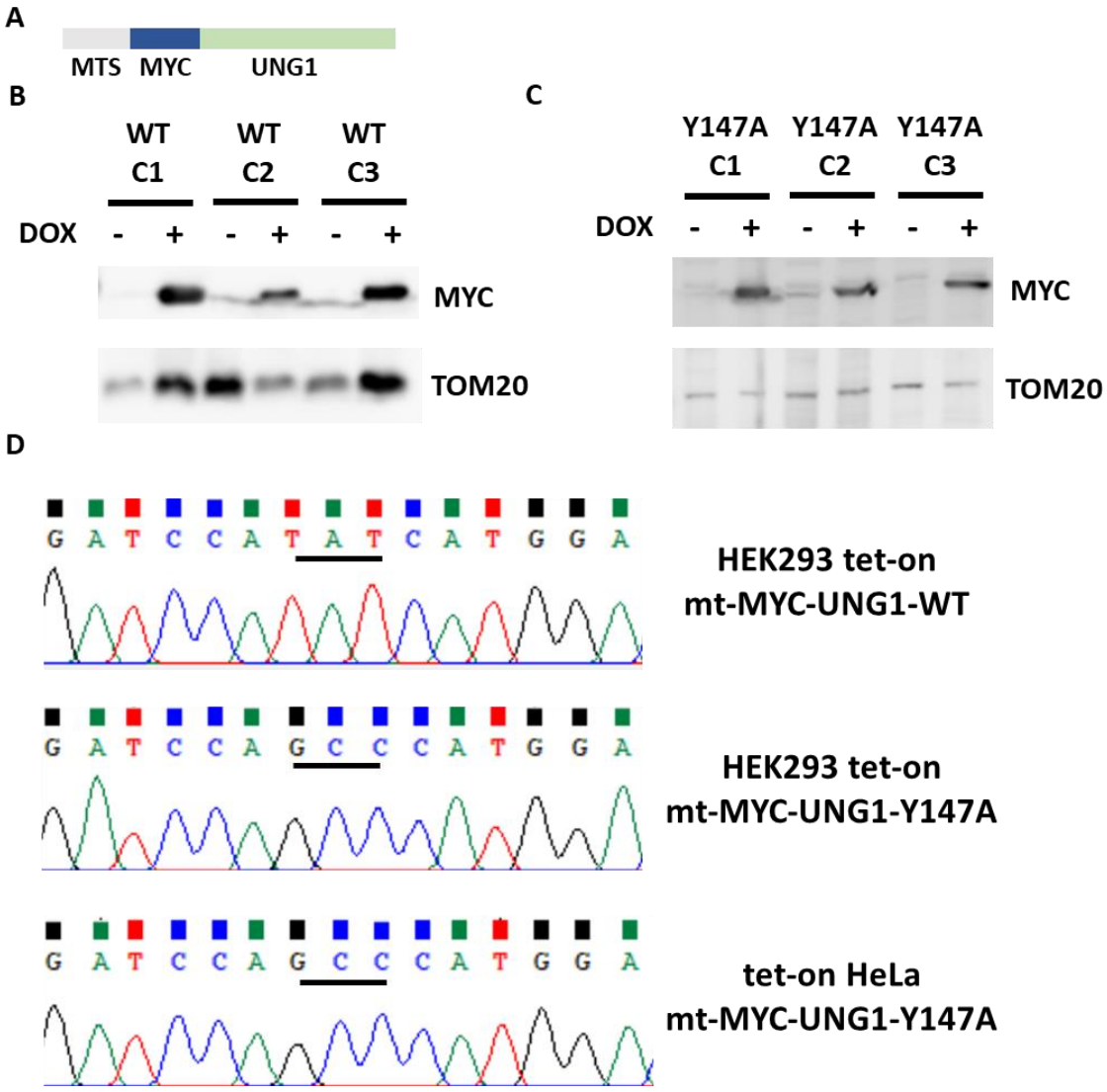

Figure 1. Mitochondrial targeting UNG1 variants transduced cell lines.

(A) The structure of mitochondria targeting uracil DNA glycosylase 1 variants. Western blot of MYC and TOM20 in the mitochondrial fraction after 24 hr with and without doxycycline induction from (A) mt-MYC-UNG1-WT transduced HEK 293 tet-on cells and (B) mt-MYC-UNG1-Y147A transduced HEK 293 tet-on cells. (C) The sequences of transduced mt-MYC-UNG1 gene in mt-MYC-UNG1-WT HEK 293 tet-on cells, mt-MYC-UNG1-Y147A transduced HEK 293 tet-on cells and mt-MYC-UNG1-Y147A transduced tet-on HeLa cells. Myc-tag (MYC).

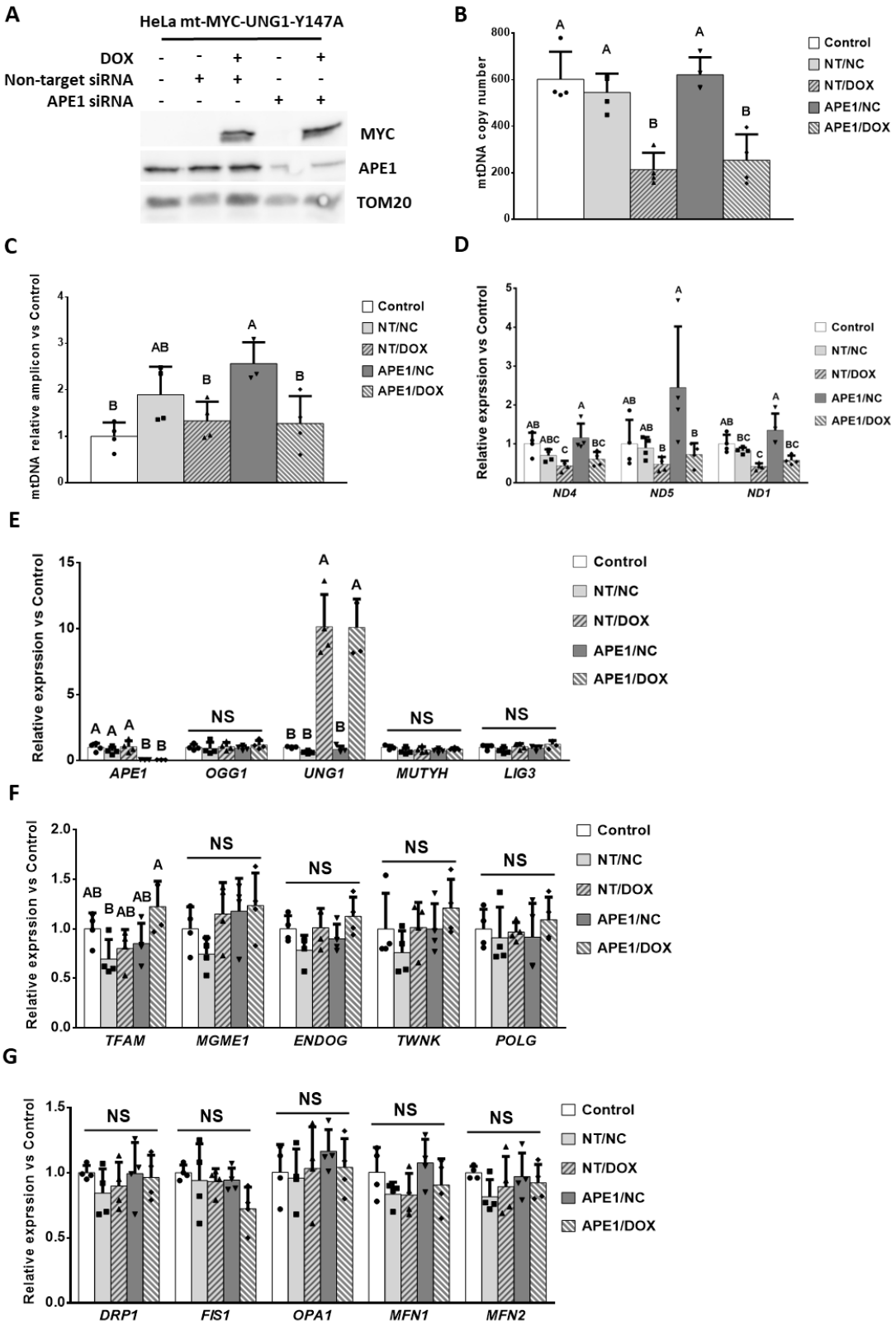
A
HeLa mt-MYC-UNG1-Y147A
DOX
Non-target siRNA
APE1 siRNA
MYC
APE1
TOM20
B
mtDNA copy number
Control
NT/NC
NT/DOX
APE1/NC
APE1/DOX
C
mtDNA relative amplicon vs Control
D
Relative exprssion vs Control
ND4
ND5
ND1
E
APE1
OGG1
UNG1
MUTYH
LIG3
NS
F
TFAM
MGME1
ENDOG
TWNK
POLG
G
DRP1
FIS1
OPA1
MFN1
MFN2

Figure 2. UNG1-Y147A overexpression and APE1 knockdown in HeLa cells.

(A) Western blot of MYC, APE1 and TOM20 in the mitochondrial fractions, (B) mtDNA copy number, (C) mtDNA relative amplicons, gene expressions of (D) mtDNA encoded genes, (E) DNA repair, (F) mitochondrial nucleoid, and (G) mitochondrial fission/fusion of tet-on HeLa UNG1-Y147A cells after 72 hr non-target or ape1 siRNA with and without 24 hr doxycycline treatment (Mean ± SD, n = 4). Different letters indicate significant difference ($p < 0.05$) between different groups by one-way ANOVA followed by Tukey's HSD test.

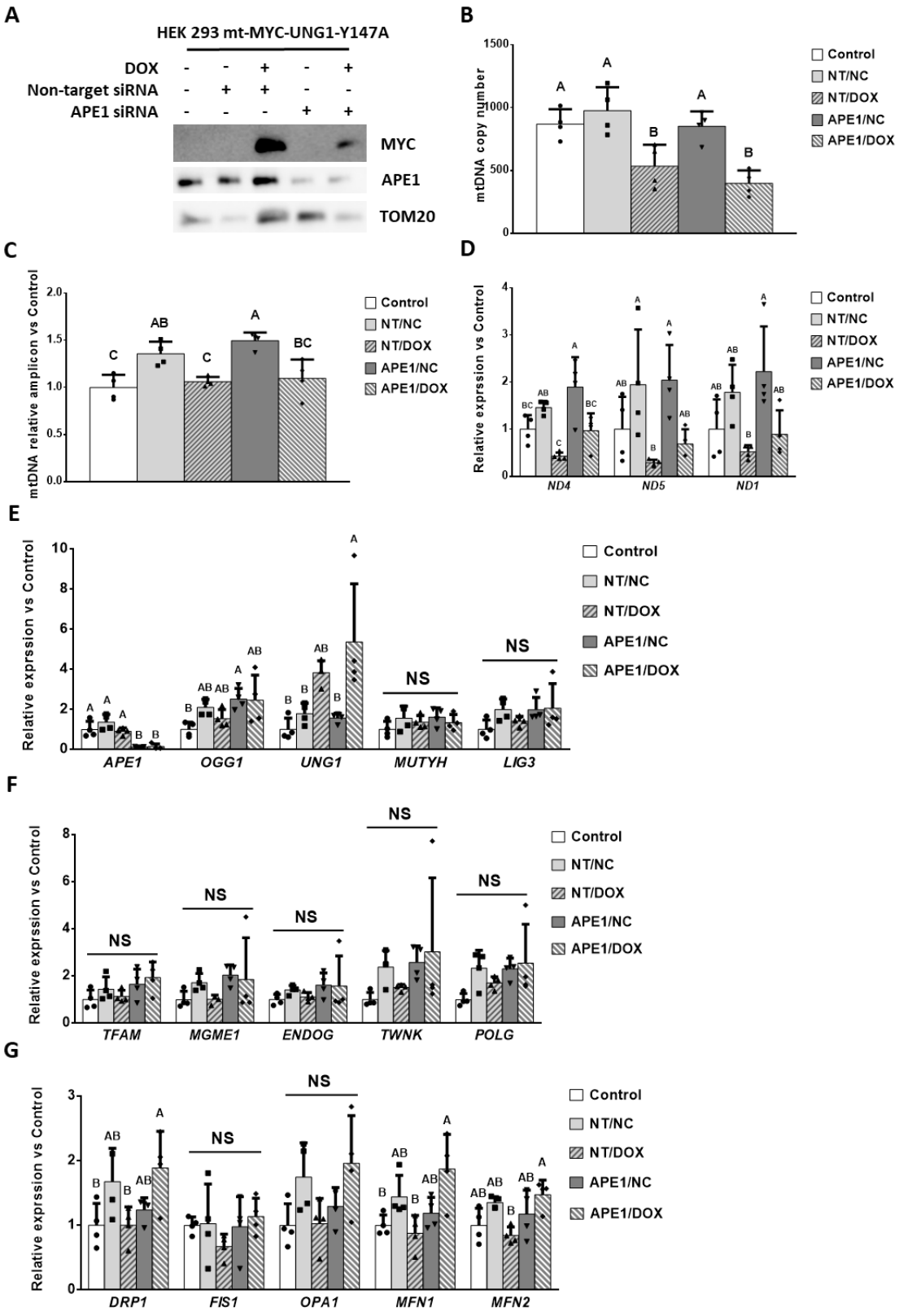
A
HEK 293 mt-MYC-UNG1-Y147A
DOX - - + - +
Non-target siRNA - + + - -
APE1 siRNA - - - + +
MYC
APE1
TOM20
B
mtDNA copy number
Control
NT/NC
NT/DOX
APE1/NC
APE1/DOX
C
mtDNA relative amplicon vs Control
D
Relative exprssion vs Control
ND4
ND5
ND1
E
Relative exprssion vs Control
APE1
OGG1
UNG1
MUTYH
LIG3
NS
F
Relative exprssion vs Control
TFAM
MGME1
ENDOG
TWNK
POLG
G
Relative exprssion vs Control
DRP1
FIS1
OPA1
MFN1
MFN2

Figure 3. UNG1-Y147A overexpression and APE1 knockdown in HEK293 cells.

(A) Western blot of MYC, APE1 and TOM20 in the mitochondrial fractions, (B) mtDNA copy number, (C) mtDNA relative amplicons, gene expressions of (D) mtDNA encoded genes, (E) DNA repair, (F) mitochondrial nucleoid, and (G) mitochondrial fission/fusion of HEK293 tet-on UNG1-Y147A cells after 72 hr non-target or ape1 siRNA with and without 24 hr doxycycline treatment (Mean ± SD, n = 4). Different letters indicate significant difference ($p < 0.05$) between different groups by one-way ANOVA followed by Tukey's HSD test.

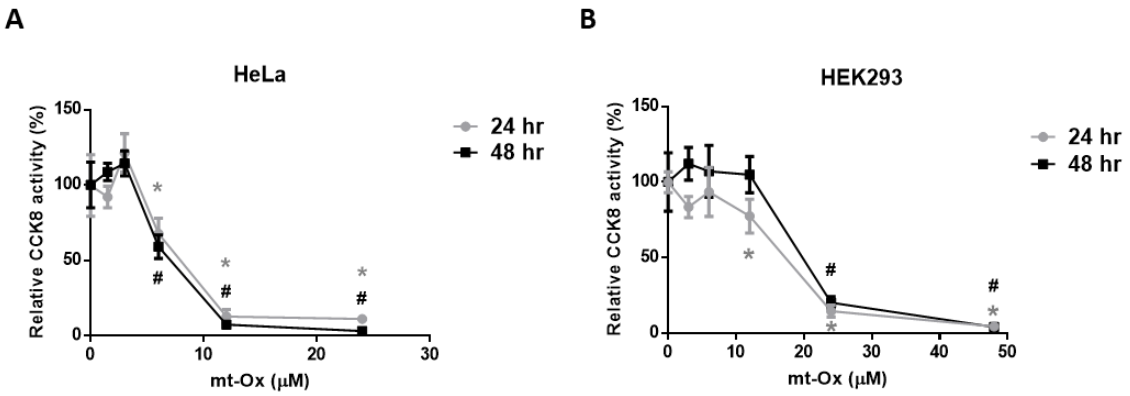

Figure 4. LC_{50} of mt-Ox.
The CCK-8 activity of (A) tet-on HeLa cells and (B) HEK293 tet-on cells after 24 hr and 48 hr of mt-Ox treatment or vehicle control (0.5% DMSO) (Mean ± SD, n = 5). Asterisk indicates significant difference vs 24 hr VC and hashtag indicates significant difference vs 48 hr VC by One-way ANOVA followed by Tuckey's HSD test.

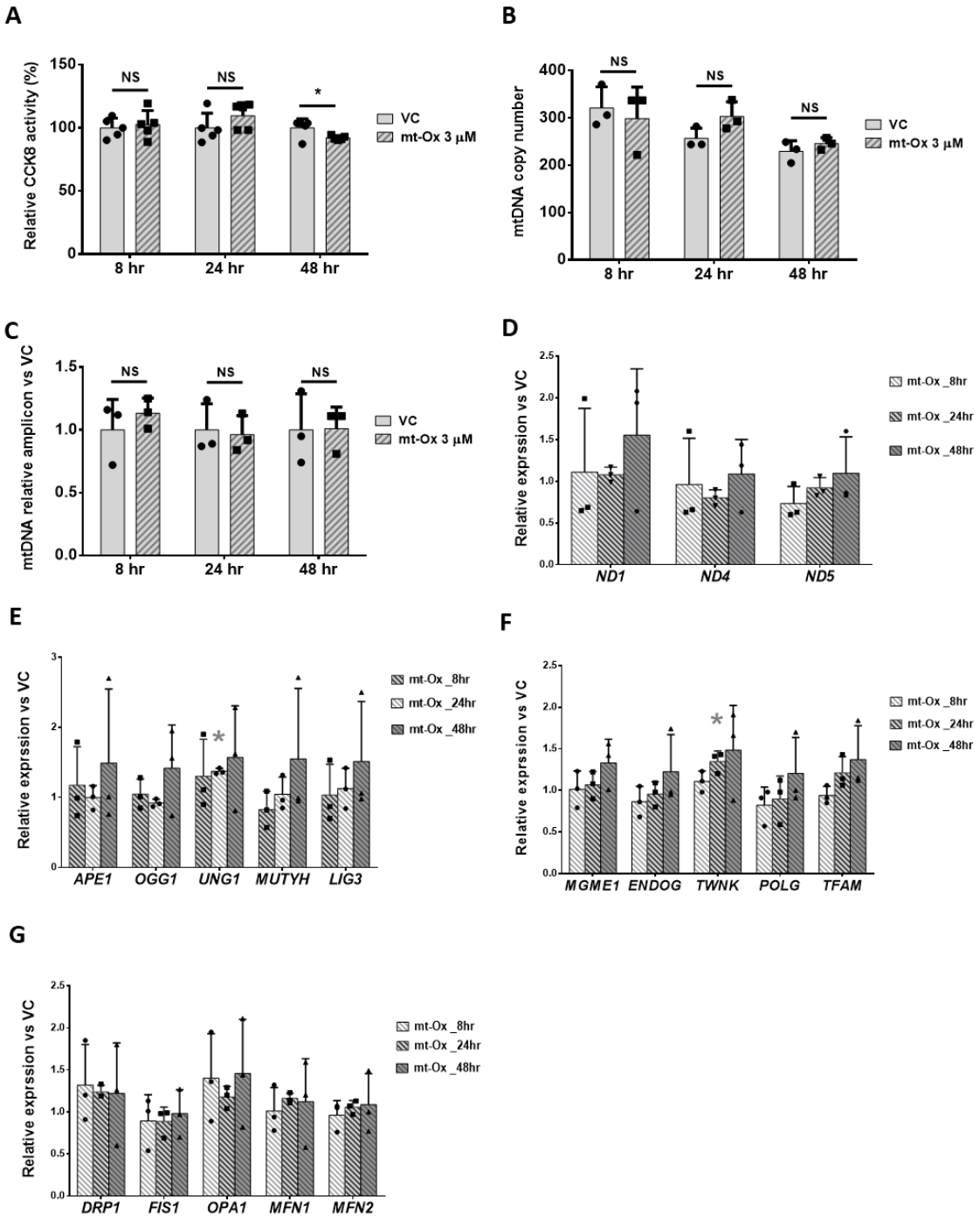
A
Relative CCK8 activity (%)
150
100
50
0
NS
NS
*
8 hr
24 hr
48 hr
VC
mt-Ox 3 μM
B
mtDNA copy number
400
300
200
100
0
NS
NS
NS
8 hr
24 hr
48 hr
VC
mt-Ox 3 μM
C
mtDNA relative amplicon vs VC
1.5
1.0
0.5
0.0
NS
NS
NS
8 hr
24 hr
48 hr
VC
mt-Ox 3 μM
D
Relative exprssion vs VC
2.5
2.0
1.5
1.0
0.5
0.0
ND1
ND4
ND5
mt-Ox _8hr
mt-Ox _24hr
mt-Ox _48hr
E
Relative exprssion vs VC
3
2
1
0
*
APE1
OGG1
UNG1
MUTYH
LIG3
mt-Ox _8hr
mt-Ox _24hr
mt-Ox _48hr
F
Relative exprssion vs VC
2.5
2.0
1.5
1.0
0.5
0.0
*
MGME1
ENDOG
TWNK
POLG
TFAM
mt-Ox _8hr
mt-Ox _24hr
mt-Ox _48hr
G
Relative exprssion vs VC
2.5
2.0
1.5
1.0
0.5
0.0
DRP1
FIS1
OPA1
MFN1
MFN2
mt-Ox _8hr
mt-Ox _24hr
mt-Ox _48hr

Figure 5. HeLa cells with 3 μM mt-Ox treatment.
The CCK-8 activity, (B) mtDNA copy number, (C) mtDNA relative amplicons, gene expressions of (D) mtDNA encoded genes, (E) DNA repair, (F) mitochondrial nucleoid, and (G) mitochondrial fission/fusion of tet-on HeLa cells after 8, 24 and 48 hr of mt-Ox (3 μM) treatment or vehicle control (0.1% DMSO) (Mean ± SD, n = 3). Asterisk indicates significant difference vs vehicle control at $p < 0.05$ by Student's T-test.

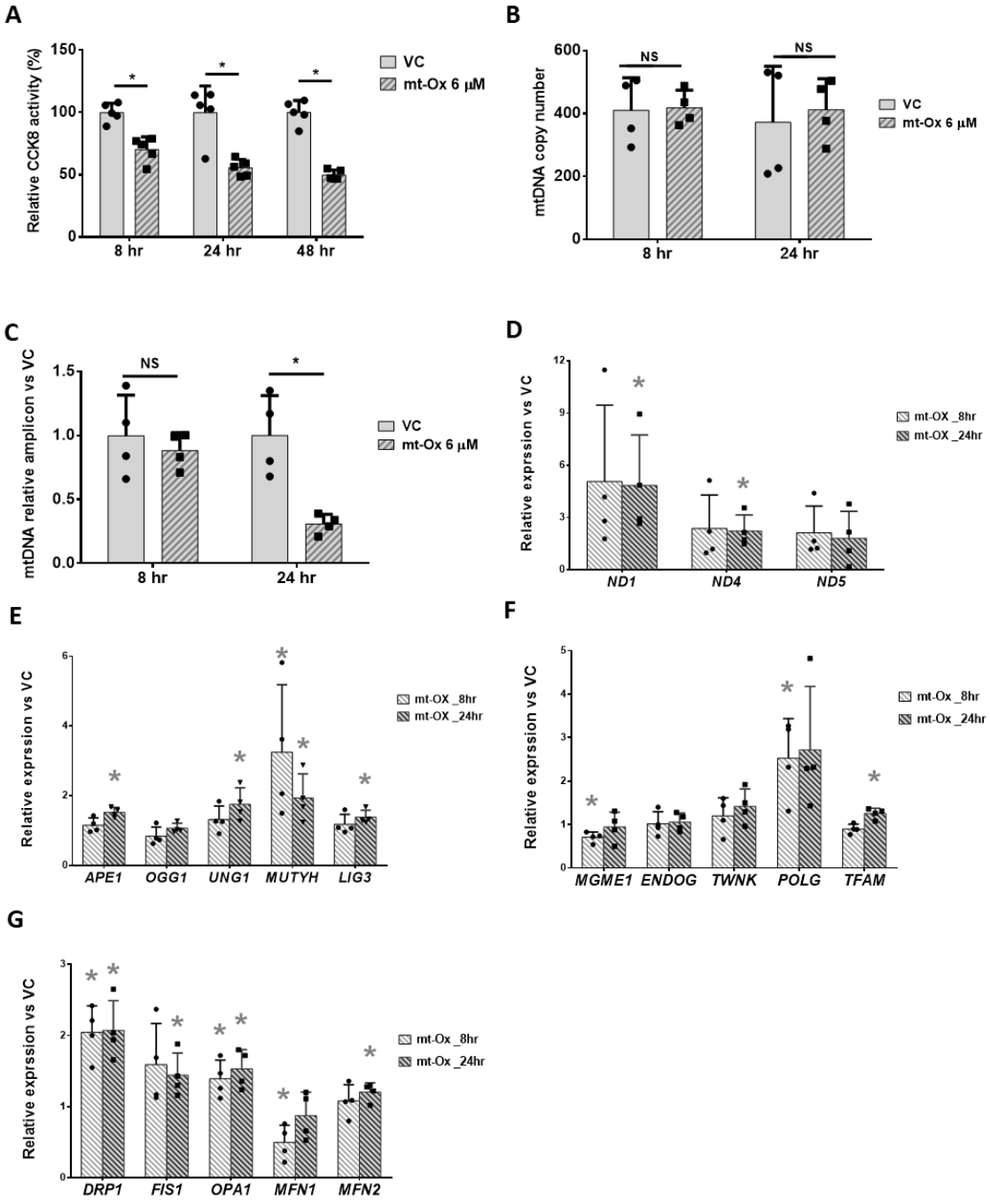
A
Relative CCK8 activity (%)
150
100
50
0
8 hr
24 hr
48 hr
VC
mt-Ox 6 µM
B
mtDNA copy number
600
400
200
0
NS
NS
8 hr
24 hr
VC
mt-Ox 6 µM
C
mtDNA relative amplicon vs VC
1.5
1.0
0.5
0.0
NS
8 hr
24 hr
VC
mt-Ox 6 µM
D
Relative exprssion vs VC
ND1
ND4
ND5
mt-OX _8hr
mt-OX _24hr
E
Relative exprssion vs VC
APE1
OGG1
UNG1
MUTYH
LIG3
mt-OX _8hr
mt-OX _24hr
F
Relative exprssion vs VC
MGME1
ENDOG
TWNK
POLG
TFAM
mt-Ox _8hr
mt-Ox _24hr
G
Relative exprssion vs VC
DRP1
FIS1
OPA1
MFN1
MFN2
mt-Ox _8hr
mt-Ox _24hr

Figure 6. HeLa cells with 6 μM mt-Ox treatment.
(A) The CCK-8 activity, (B) mtDNA copy number, (C) mtDNA relative amplicons, gene expressions of (D) mtDNA encoded genes, (E) DNA repair, (F) mitochondrial nucleoid, and (G) mitochondrial fission/fusion of tet-on HeLa cells after 8, 24 and 48 hr of mt-Ox (3 μM) treatment or vehicle control (0.1% DMSO) (Mean ± SD, n = 4). Asterisk indicates significant difference vs vehicle control at $p < 0.05$ by Student's T-test.

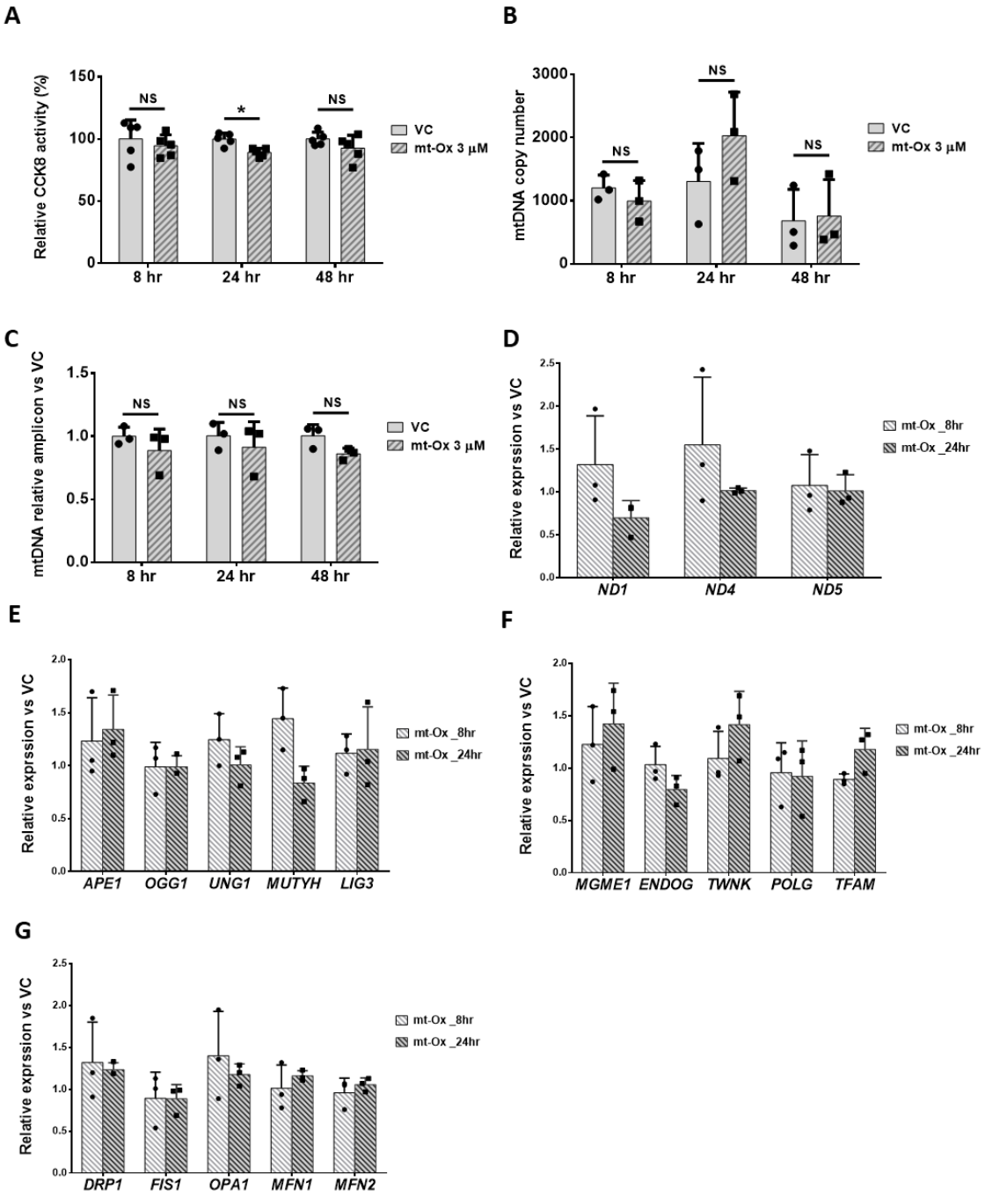
A
Relative CCK8 activity (%)
150
100
50
0
NS
*
NS
8 hr
24 hr
48 hr
VC
mt-Ox 3 μM
B
mtDNA copy number
3000
2000
1000
0
NS
NS
NS
8 hr
24 hr
48 hr
VC
mt-Ox 3 μM
C
mtDNA relative amplicon vs VC
1.5
1.0
0.5
0.0
NS
NS
NS
8 hr
24 hr
48 hr
VC
mt-Ox 3 μM
D
Relative exprssion vs VC
2.5
2.0
1.5
1.0
0.5
0.0
ND1
ND4
ND5
mt-Ox _8hr
mt-Ox _24hr
E
Relative exprssion vs VC
2.0
1.5
1.0
0.5
0.0
APE1
OGG1
UNG1
MUTYH
LIG3
mt-Ox _8hr
mt-Ox _24hr
F
Relative exprssion vs VC
2.0
1.5
1.0
0.5
0.0
MGME1
ENDOG
TWNK
POLG
TFAM
mt-Ox _8hr
mt-Ox _24hr
G
Relative exprssion vs VC
2.5
2.0
1.5
1.0
0.5
0.0
DRP1
FIS1
OPA1
MFN1
MFN2
mt-Ox _8hr
mt-Ox _24hr

Figure 7. HEK293 cells with 3 μM mt-Ox treatment.
(A) The CCK-8 activity, (B) mtDNA copy number, (C) mtDNA relative amplicons, gene expressions of (D) mtDNA encoded genes, (E) DNA repair, (F) mitochondrial nucleoid, and (G) mitochondrial fission/fusion of HEK293 tet-on cells after 8, 24 and 48 hr of mt-Ox (3 μM) treatment or vehicle control (0.1% DMSO) (Mean ± SD, n = 3). Asterisk indicates significant difference vs vehicle control at $p < 0.05$ by Student's T-test.

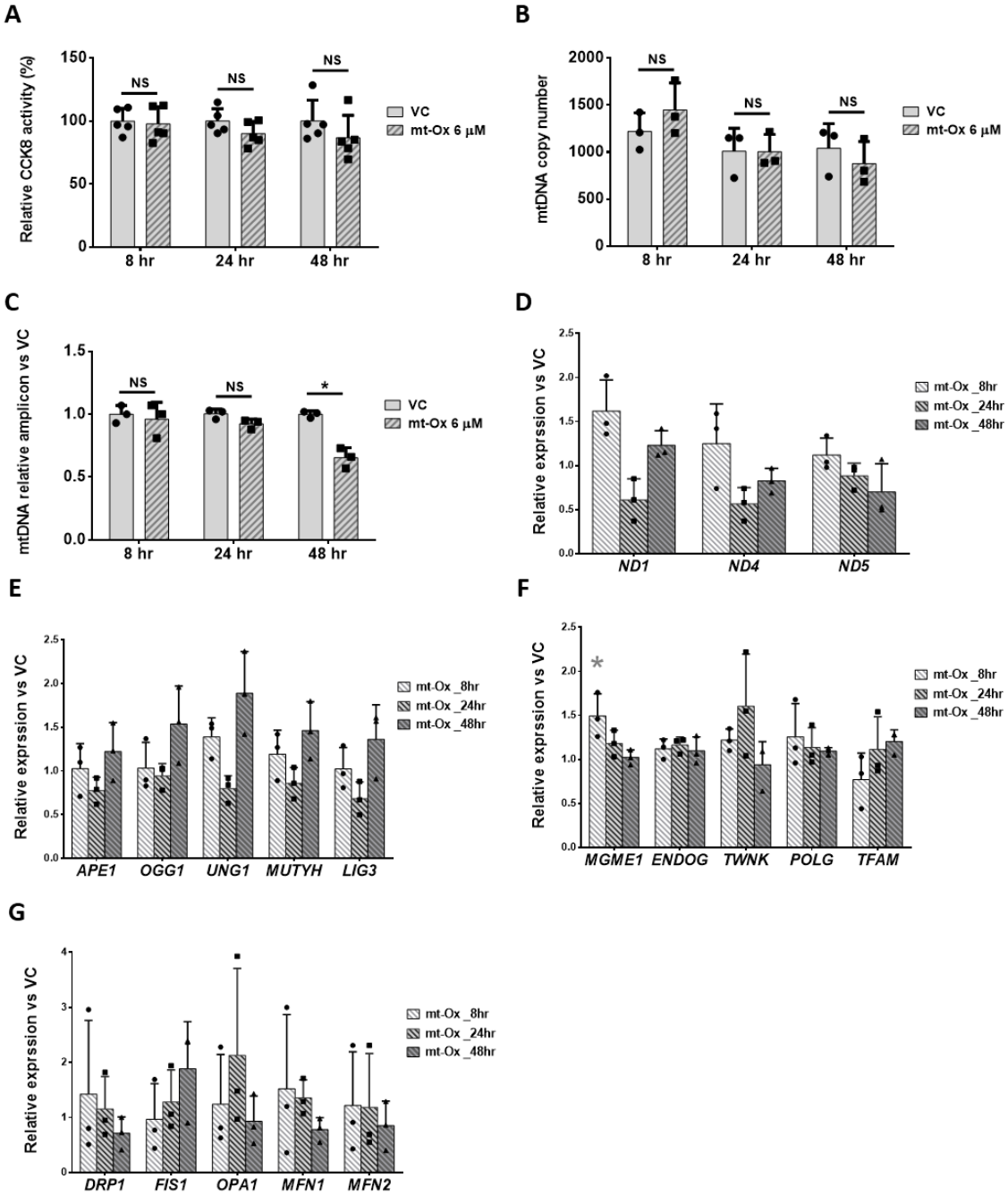
A
Relative CCK8 activity (%)
150
100
50
0
NS
NS
NS
8 hr
24 hr
48 hr
VC
mt-Ox 6 μM
B
mtDNA copy number
2000
1500
1000
500
0
NS
NS
NS
8 hr
24 hr
48 hr
VC
mt-Ox 6 μM
C
mtDNA relative amplicon vs VC
1.5
1.0
0.5
0.0
NS
NS
*
8 hr
24 hr
48 hr
VC
mt-Ox 6 μM
D
Relative exprssion vs VC
2.5
2.0
1.5
1.0
0.5
0.0
ND1
ND4
ND5
mt-Ox _8hr
mt-Ox _24hr
mt-Ox _48hr
E
Relative exprssion vs VC
2.5
2.0
1.5
1.0
0.5
0.0
APE1
OGG1
UNG1
MUTYH
LIG3
mt-Ox _8hr
mt-Ox _24hr
mt-Ox _48hr
F
Relative exprssion vs VC
2.5
2.0
1.5
1.0
0.5
0.0
*
MGME1
ENDOG
TWNK
POLG
TFAM
mt-Ox _8hr
mt-Ox _24hr
mt-Ox _48hr
G
Relative exprssion vs VC
4
3
2
1
0
DRP1
FIS1
OPA1
MFN1
MFN2
mt-Ox _8hr
mt-Ox _24hr
mt-Ox _48hr

Figure 8. HEK293 cells with 6 μM mt-Ox treatment.
(A) The CCK-8 activity, (B) mtDNA copy number, (C) mtDNA relative amplicons, gene expressions of (D) mtDNA encoded genes, (E) DNA repair, (F) mitochondrial nucleoid, and (G) mitochondrial fission/fusion of HEK293 tet-on cells after 8, 24 and 48 hr of mt-Ox (6 μM) treatment or vehicle control (0.1% DMSO) (Mean ± SD, n = 3). Asterisk indicates significant difference vs vehicle control at $p < 0.05$ by Student's T-test.

Appendix

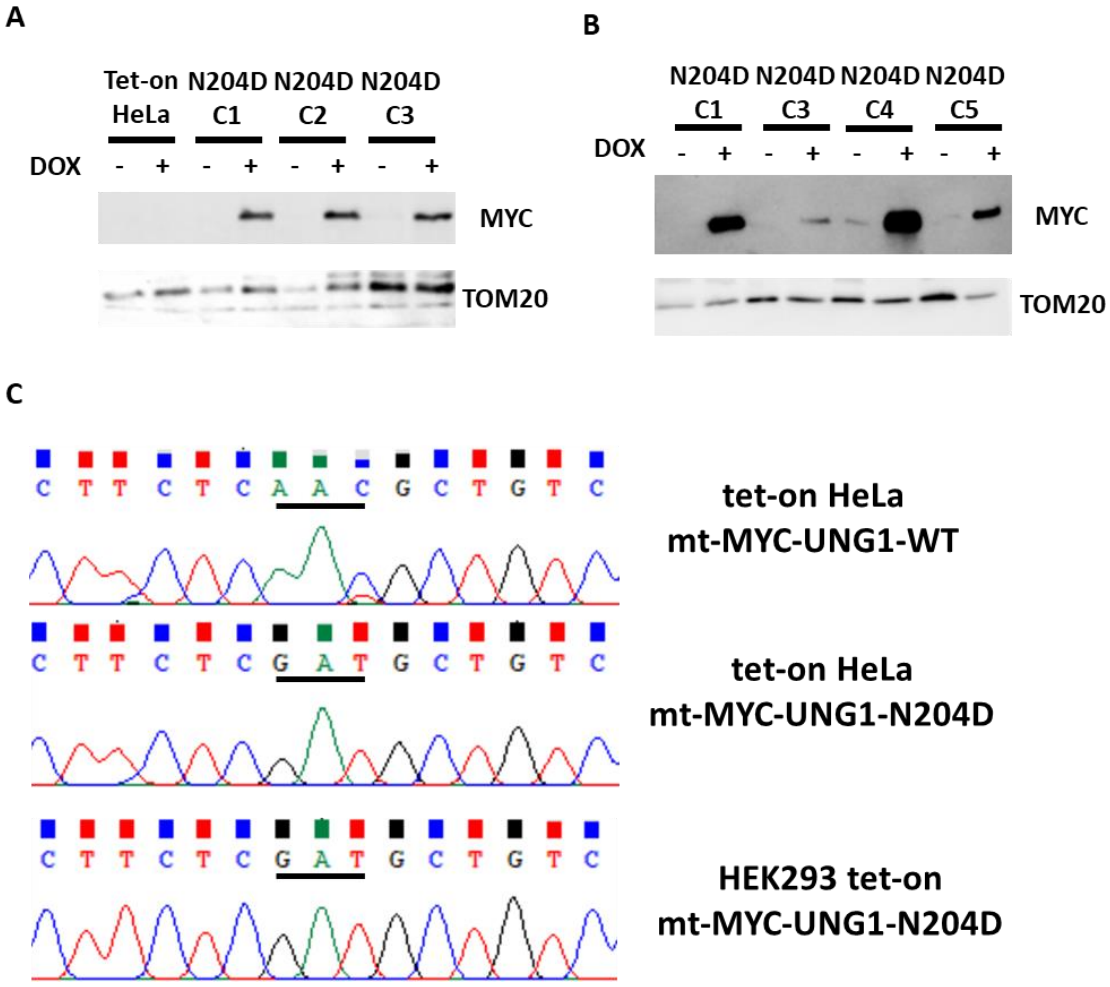

Figure S1. Validation of UNG1-N204D transduced cell lines.

Western blot of MYC and TOM20 in the mitochondrial fraction after 24 hr with and without doxycycline induction from (A) mt-MYC-UNG1-N204D transduced tet-on HeLa cells and (B) mt-MYC-UNG1-N204D transduced HEK 293 tet-on cells. (C) The sequences of transduced mt-MYC-UNG1 gene in mt-MYC-UNG1-WT tet-on HeLa, mt-MYC-UNG1-N204D tet-on HeLa and mt-MYC-UNG1-N204D HEK 293 tet-on cells.

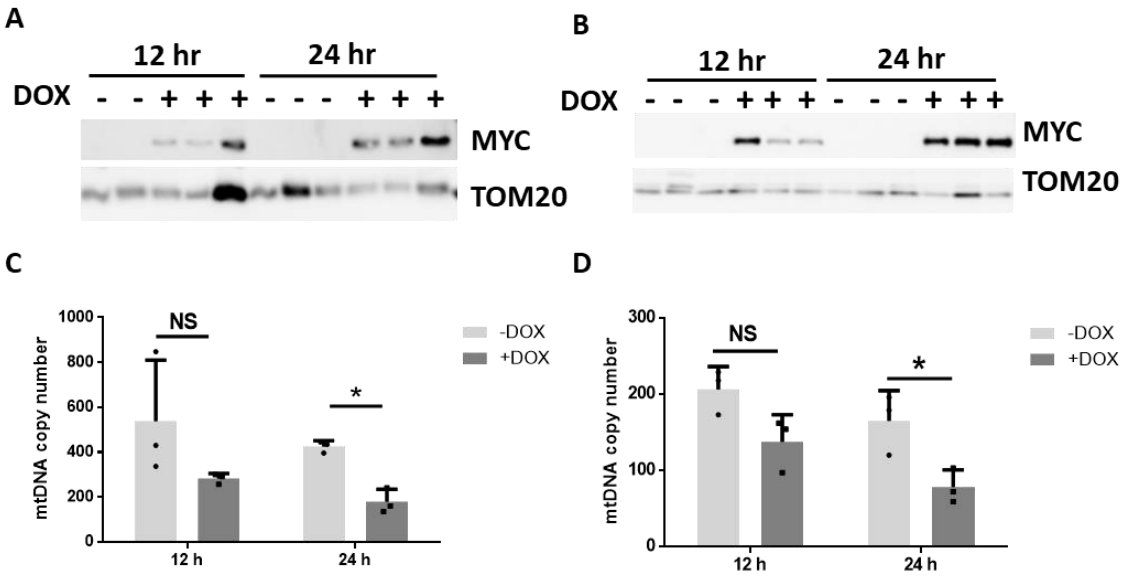

Figure S2. mtDNA copy number of UNG1-N204D transduced cell lines.
Western blot of MYC and TOM20 in the mitochondrial fraction after 12 or 24 hr with and without doxycycline induction from mt-MYC-UNG1-N204D transduced tet-on HeLa cell line (A) colony 1 and (B) colony 2. The mtDNA copy number in the mt-MYC-UNG1-N204D transduced tet-on HeLa cell line (C) colony 1 and (D) colony 2 after 12 or 24 hr with and without doxycycline induction (Mean ± SD, n = 3). Asterisk indicates significant difference ($p < 0.05$) between the cells with and without doxycycline induction by Student's t-test.

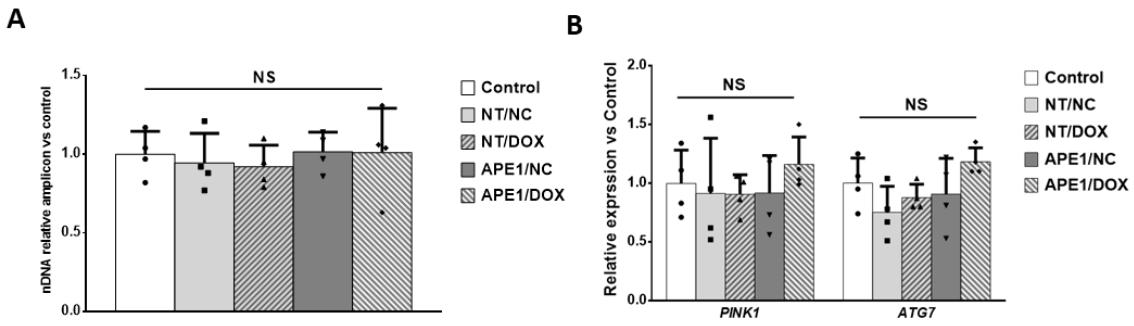

Figure S3. UNG1-Y147A overexpression and APE1 knockdown in HeLa cells.
(A) nDNA relative amplicons and (B) mitophagy related gene expressions of tet-on HeLa UNG1-Y147A cells after 72 hr non-target or ape1 siRNA with and without 24 hr doxycycline treatment (Mean ± SD, n = 4). Different letters indicate significant difference ($p < 0.05$) between different groups by one-way ANOVA followed by Tukey's HSD test.

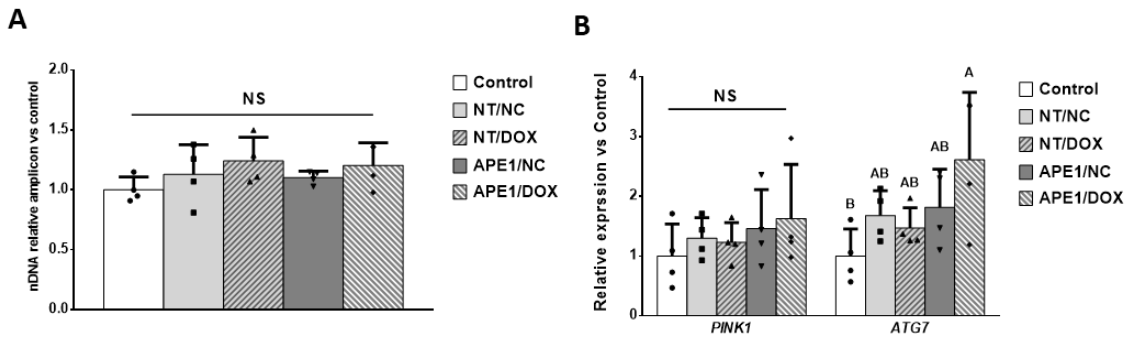

Figure S4. UNG1-Y147A overexpression and APE1 knockdown in HEK293 cells.
(A) nDNA relative amplicons and (B) mitophagy related gene expressions of HEK293 tet-on UNG1-Y147A cells after 72 hr non-target or ape1 siRNA with and without 24 hr doxycycline treatment (Mean ± SD, n = 4). Different letters indicate significant difference ($p < 0.05$) between different groups by one-way ANOVA followed by Tukey's HSD test.

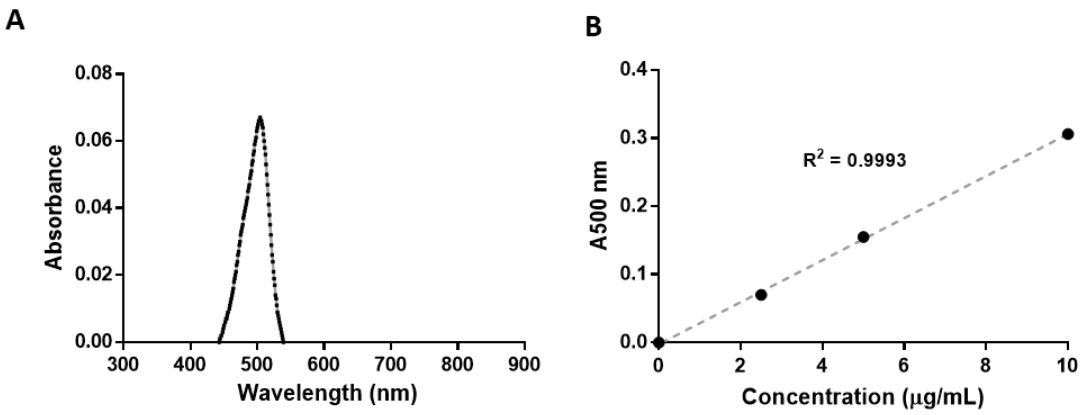

Figure S5. The light absorbance of mt-Ox.
(A) The absorbance of mt-Ox (5 μg/mL) at different wavelength. (B) The 500 nm absorbance of 0-10 μg/mL mt-Ox.

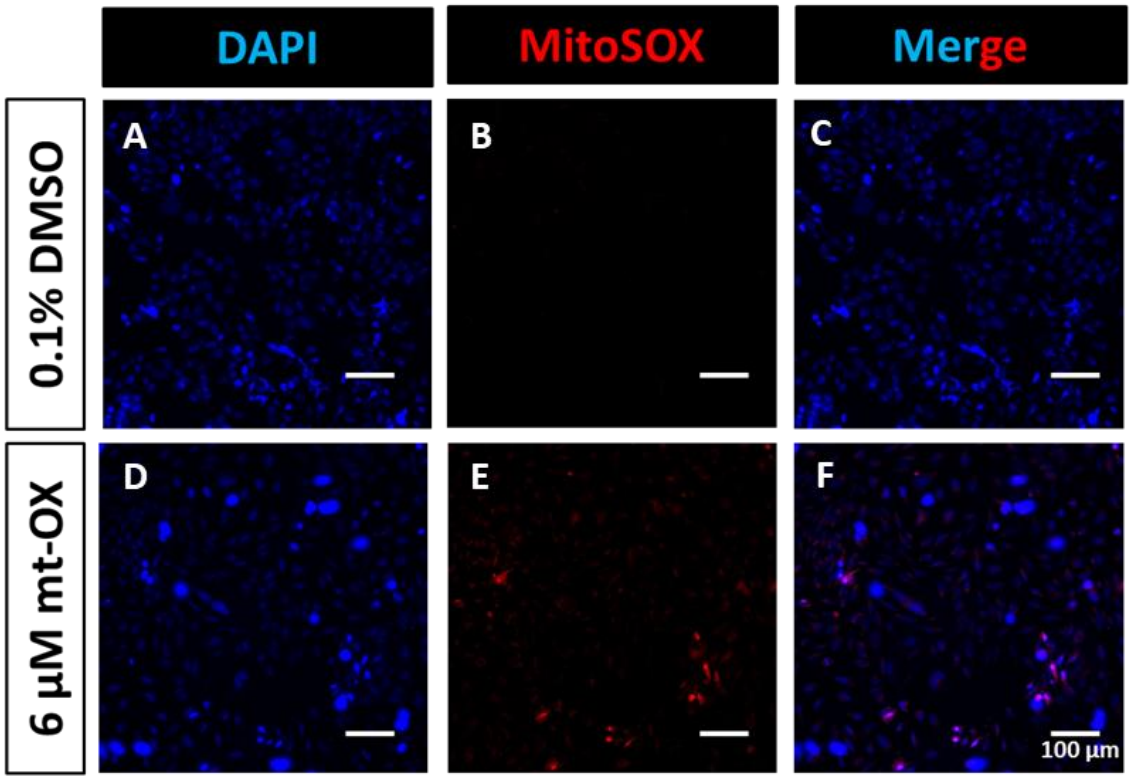

Figure S6. MitoSOX staining of mt-Ox-treated HeLa cells.
(A) DAPI, (B) MitoSOX and (C) the merge of DAPI and MitoSOX signals in tet-on HeLa cells after 48 hr of vehicle control (0.1% DMSO) treatment. (D) DAPI, (E) MitoSOX and (F) the merge of DAPI and MitoSOX signals in tet-on HeLa cells after 48 hr of mt-Ox (6 µM) treatment.

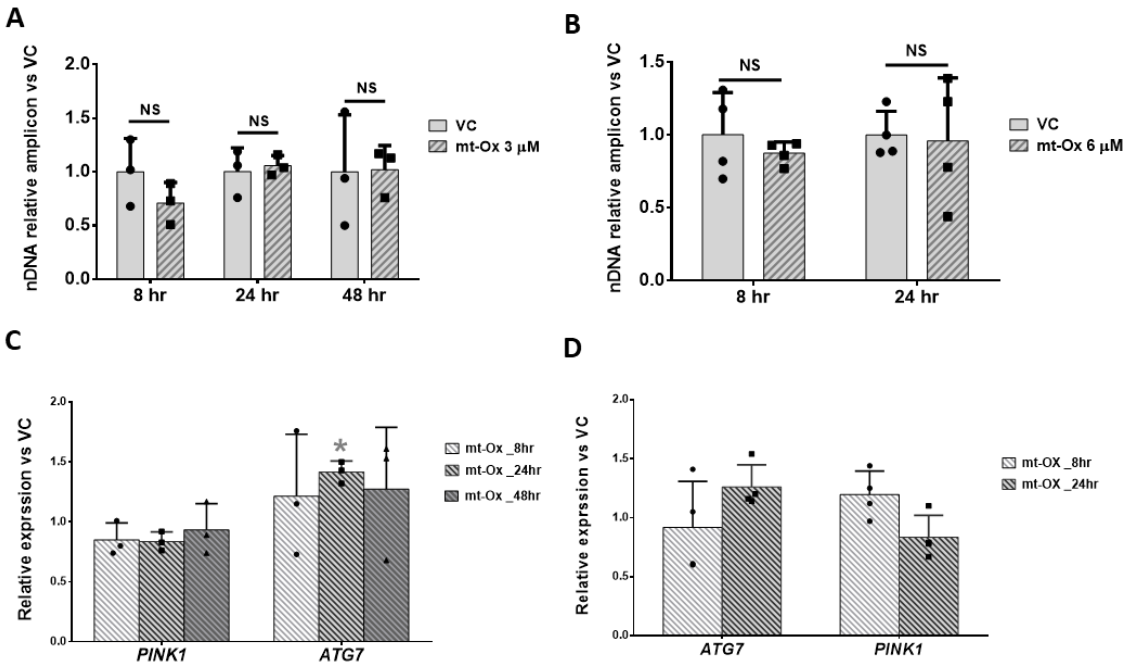

Figure S7. HeLa cells with mt-Ox treatment.
(A) The nDNA relative amplicons and (C) mitophagy related gene expressions of tet-on HeLa cells after 8, 24 and 48 hr of mt-Ox (3 μM) treatment or vehicle control (0.1% DMSO) (Mean ± SD, n = 3). (B) nDNA relative amplicons and (D) mitophagy related gene expressions of tet-on HeLa cells after 8 and 24 hr of mt-Ox (6 μM) treatment or vehicle control (0.1% DMSO) (Mean ± SD, n = 4). Asterisk indicates significant difference vs vehicle control at $p < 0.05$ by Student's T-test.

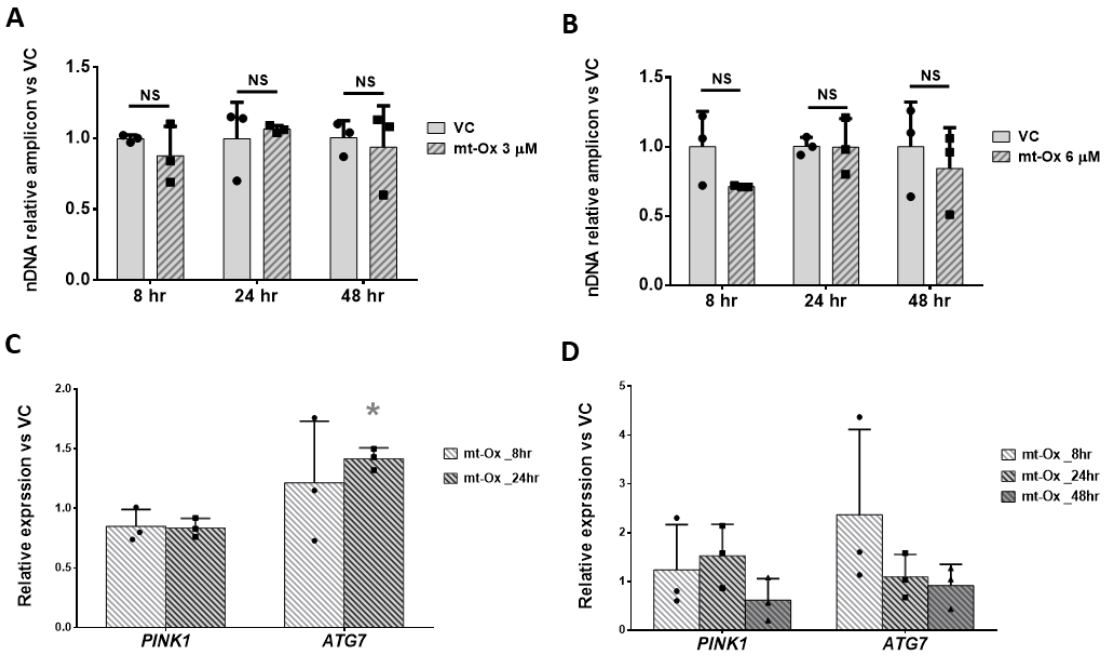

Figure S8. HEK293 cells with mt-Ox treatment.
(A) The nDNA relative amplicons and (C) mitophagy related gene expressions of HEK293 tet-on cells after 8, 24 and 48 hr of mt-Ox (3 μM) treatment or vehicle control (0.1% DMSO) (Mean ± SD, n = 3). (B) The nDNA relative amplicons and (D) mitophagy related gene expressions of HEK293 tet-on cells after 8, 24 and 48 hr of mt-Ox (6 μM) treatment or vehicle control (0.1% DMSO) (Mean ± SD, n = 3). Asterisk indicates significant difference vs vehicle control at $p < 0.05$ by Student's T-test.